

www.acsabm.org Review

Prediction and Control in DNA Nanotechnology

Marcello DeLuca, Sebastian Sensale, Po-An Lin, and Gaurav Arya*



Cite This: https://doi.org/10.1021/acsabm.2c01045

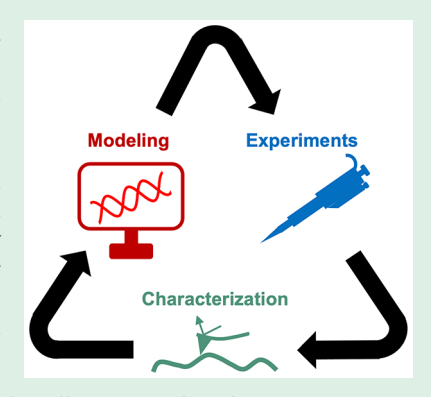


ACCESS

Metrics & More

Article Recommendations

ABSTRACT: DNA nanotechnology is a rapidly developing field that uses DNA as a building material for nanoscale structures. Key to the field's development has been the ability to accurately describe the behavior of DNA nanostructures using simulations and other modeling techniques. In this Review, we present various aspects of prediction and control in DNA nanotechnology, including the various scales of molecular simulation, statistical mechanics, kinetic modeling, continuum mechanics, and other prediction methods. We also address the current uses of artificial intelligence and machine learning in DNA nanotechnology. We discuss how experiments and modeling are synergistically combined to provide control over device behavior, allowing scientists to design molecular structures and dynamic devices with confidence that they will function as intended. Finally, we identify processes and scenarios where DNA nanotechnology lacks sufficient prediction ability and suggest possible solutions to these weak areas.



KEYWORDS: DNA nanotechnology, DNA origami, simulations, molecular dynamics, artificial intelligence, machine learning, statistical mechanics, kinetic modeling

■ INTRODUCTION

DNA nanotechnology¹ is a field that uses the canonical base-pairing rules of DNA to rationally program its self-assembly into nanoscale structures. Over the past 40 years of the field's development, DNA nanotechnology has enabled scientists to make advancements in diagnostics,² therapeutics,³ metrology,⁴ computation,⁵ photonics,⁶ and other applications.⁷ DNA nanotechnology's best-known design paradigm, DNA origami,⁸ is emerging as a highly versatile tool for creating elaborate devices for investigating nanoscale and microscale phenomena, which are leading to applications that would not have been foreseen even a decade ago.

Key to many of these developments has been an increasing capability of prediction and control, which fall largely into the domain of modeling. Every technology that finds its way into long-term use has relied upon the ability to predict behavior given a set of inputs and thus control system behavior by optimizing those inputs. DNA nanotechnology is no different, and scientists can now use it purely as a tool for investigations that have little to do with the technology itself. This has been enabled largely by the advent of modeling techniques, which can reliably predict the outcomes of correct DNA structure folding;^{9,10} availability of various biochemical-biophysical tools for characterizing DNA structure and properties; 11 and greater understanding of fundamental processes such as toeholdmediated strand displacement, ¹² change in form of DNA, ^{13–15} etc. As time goes on and DNA nanotechnology begins to be relied upon for commercial applications in potentially highcost industries such as healthcare, 16,17 the value of quantitative

understanding of DNA nanotechnology will surely increase. However, the field currently lacks a comprehensive description of the available modeling paradigms and opportunities to improve our ability to predict experimental outcomes. In this Review, we will describe the various modeling techniques used in this field and how they are used to predict device behavior, which ultimately affords control over DNA nanotechnology. We will also identify underutilized modeling techniques as well as areas where modeling is currently insufficient and therefore hinders the progress of DNA nanotechnology.

The span of length and time scales relevant to DNA nanotechnology is enormous. At the smallest scale, bond vibrations occur on a time scale of femtoseconds. Base-pair fluctuations occur on a time scale of nanoseconds and length scale of angstroms. Hybridization of tens of nucleotides can take milliseconds for individual hybridization events on partially hybridized strands and seconds to minutes for separated strands to hybridize in bulk solution at physically relevant concentrations. The self-assembly of DNA structures thousands of nucleotides in size takes seconds to a few hours and spans tens to hundreds of nanometers, and hierarchical assembly and larger-scale organization of giga-

Special Issue: Computational Advances in Biomaterials

Received: December 15, 2022 Accepted: February 9, 2023



dalton-scale DNA assemblies can take from a few to several hours and span from hundreds of nanometers to micrometers. To further complicate matters, some components of DNA nanotechnology behave rigidly where they can be modeled as continuum bodies, while others exhibit significant thermally driven stochasticity that is best described using statistical treatments.

Unsurprisingly, there is not a single modeling technique that can capture the full span of these behaviors, and some compromise must be made between detail/resolution and time/length scale when conducting simulations. In this Review, we will categorize modeling techniques by resolution into quantum mechanics, all-atom, coarse-grained, mesoscopic, and continuum resolution models and describe the utility and limitations of each. We will also describe the different simulation techniques available for each of these models, including explicit-solvent molecular dynamics, Brownian dynamics, rigid-body dynamics, finite element analysis, statistical mechanics theory, kinetic modeling, and machine learning to determine experimental or simulation observables; we will also describe existing techniques, which span multiple resolution or simulation paradigms. A diagram of where some of these modeling techniques fit into DNA nanotechnology's span of length and time scales can be found in Figure 1. We

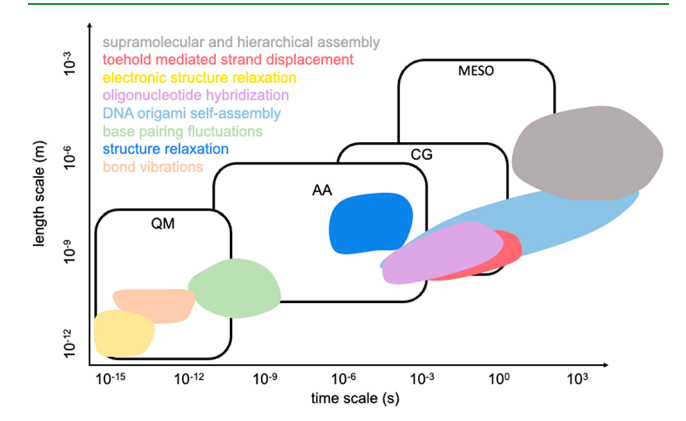


Figure 1. Length and time scales of features and processes in DNA nanotechnology and the length and time scales practically accessible by different modeling techniques, including quantum mechanics calculations ("QM"), all-atom molecular dynamics simulations ("AA"), coarse-grained simulations ("CG"), and mesoscopic modeling ("MESO"). Shape representations for each dynamic process type are not precise but aim to generally capture their range.

will describe how simulations and experiments are compared to refine models and improve predictive power. Finally, we will describe grand challenges in the field and propose some solutions to those challenges.

RESOLUTIONS OF MODELING AND SIMULATION TECHNIQUES

Quantum Mechanics (QM). In QM simulations, the Schrödinger equation is approximately solved for the time-independent many-electron case to obtain the electronic distributions of all species in the system. Density Functional Theory²⁷ (DFT) is the most common technique used for this purpose. DFT replaces the many body wave functions $\Psi(\mathbf{r}_1, \mathbf{r}_2, ... \mathbf{r}_N)$ of a system, where \mathbf{r}_i denotes the Cartesian coordinates of individual bodies, with a single spatial electronic density $n(\mathbf{r})$, which is notably a function of a single set of Cartesian

coordinates; the many other properties of the system such as potentials and energy gradients may then be expressed as functionals of $n(\mathbf{r})$. Interaction forces computed by using this method can also be propagated in time and used to simulate system dynamics in a method known as ab initio molecular dynamics.²⁸

The above formalism contains all of the nuance of multibody effects, nonspherical interactions, chemical reactivity, and electron transport, so in theory it should accurately reproduce the structural and dynamic behavior of DNA nanodevices. However, the schemes employed to calculate these electronic structures are extremely computationally expensive, so the use of QM in direct simulation of DNA origami devices has been mostly limited to the study of very specific aspects, such as electron transfer in single- and double-stranded DNA, 29-32 the formation of G-quadruplexes,³³ the impact of polarization effects on ionic binding to DNA quadruplexes,³⁴ and QM studies of basic DNA features such as hydrogen bonding,³⁵ base stacking,³⁶ and ionic binding in canonically bound DNA.³⁷ A less apparent yet more pervasive way that QM simulations have impacted DNA nanotechnology is through their role in parametrizing classical force fields of DNA, ions, and water molecules commonly used in all-atom molecular dynamics (AAMD) simulations. 38 Interestingly, the advent of quantum computing may eventually make it possible to rapidly compute electronic structure and conduct quantum mechanics-based simulations at significantly lower cost, which could open the doors for new modeling paradigms.3

All-Atom Molecular Dynamics (AAMD) Simulations. In atomistic models, the electronic degrees of freedom, explicitly treated through QM simulations, are implicitly treated by means of semiempirical potential energy functions representing the "effective" interatomic interactions between the individual atoms of a molecular system. By propagating the classical Newton's equations of motion for every atom found in a molecular system of interest, the dynamics of the system can be simulated in physical time. The simplified treatment of interatomic interactions in AAMD simulations allows access to orders of magnitude longer time scales than is possible with QM simulations, although the accuracy of the results obtained is highly dependent on the quality of the imposed interatomic interactions (i.e., the implemented force field). Atomistic models have been utilized to study biological systems for almost 50 years, 40 and the first atomistic simulations of nucleic acid molecules were reported in the early 1980s by Levitt⁴¹ and Tidor et al.42 In these simulations, canonical B-form DNA duplexes of under 20 base pairs were simulated for tens of picoseconds with an implicit treatment of the solvent, leading to highly distorted and unreasonable conformations. Since that time, major advances in algorithms and computing hardware have drastically expanded the accuracy, sizes, and simulation times accessible with atomistic accuracy, offering fundamental insights into the structure and function of both nucleic acids and proteins.

The 1990s saw rapid development in the atomistic modeling of biological systems, as computing power allowed for the inclusion of explicit solvent in AAMD simulations. ⁴³ Different force fields such as AMBER⁴⁴ and CHARMM^{45,46} were first developed during this decade, capturing the conformational dynamics of B-form DNA duplexes over longer time scales. ^{47,48} However, the time step for numerical integration is still limited to the order of femtoseconds by the extremely fast vibrational frequency of bonds and angles involving hydrogen atoms. ⁴⁹

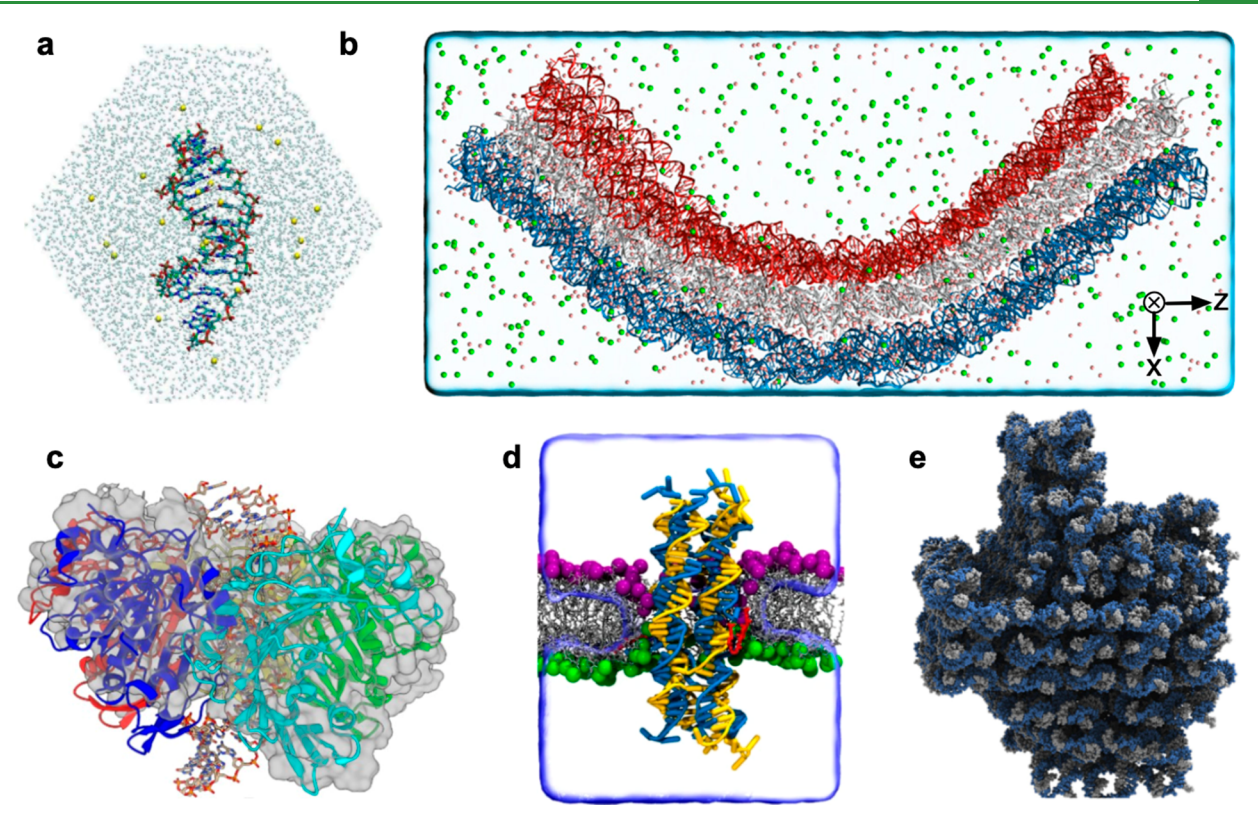


Figure 2. Applications of all-atom molecular dynamics simulations. The simulations were used for the prediction of (a) base pair and base pair step properties, (b) conformational dynamics of an 18 DNA helix bundle, (c) DNA—protein interactions, (d) cholesterol-mediated stabilization of a DNA nanostructure within a lipid bilayer, and (e) conformation of a DNA nanostructure for comparison to cryo-EM reconstruction. (a) Reproduced with permission from ref 55. Copyright 2009 Oxford University Press. (b) Reproduced with permission from ref 54. Copyright 2013 National Academy of Science. (c) Reproduced with permission from ref 56. Copyright 2021 Oxford University Press. (d) Reproduced with permission from ref 57. Copyright 2018 Springer Nature. (e) Reproduced with permission from ref 58. Copyright 2012 National Academy of Science.

Hence, a limitation of AAMD simulations is that trillions of time steps must be integrated to capture many phenomena of biological interest that occur over milliseconds, ⁵⁰ a number that challenges the capabilities of even the most advanced massively parallel supercomputers (i.e., Anton). ⁵¹

In DNA nanotechnology, AAMD can be used for producing atomically precise relaxed structures for comparison to experimental characterization techniques such as cryo-electron microscopy (cryo-EM);⁵² for more detailed mechanistic understanding of the conformations of critical components in larger DNA assemblies; and for quantifying interactions of DNA nanostructures with proteins.⁵³ Figure 2 presents several notable studies which make use of atomistic modeling and demonstrate a variety of applications of AAMD toward prediction and control in DNA-based systems. The first atomistic simulations of a DNA origami nanostructure were performed by Yoo and Aksimentiev in 2013.⁵⁴ By simulating millions of atoms including ions and water, DNA origami nanostructures approximately 50 nm long were simulated for over 100 ns, revealing significant departure of the simulated nanostructures from their idealized conformations. Explicit treatment of the solvent allows for detailed studies on the effect of the environment in the stability and local conformation of DNA origami nanostructures, \$2,59-63 while also allowing for the characterization of the ionic conductivity of DNA origami constructs such as nanopores. 57,64-68 Critically, some AAMD force fields can reasonably capture differences in interactions between DNA and monovalent ions

such as sodium versus divalent ions such as magnesium, ⁶⁹ a feature that is not present in coarser modeling techniques but can be very important to DNA nanostructure function. For example, phenomena such as magnesium-mediated DNA form change may be captured with AAMD simulations⁷⁰ but would not be captured with an implicit solvent model, which does not account for ionic size, correlation effects, and coordination. Finally, noncanonical DNA motifs, which might not be captured using coarse-grained models, can often be captured with atomistic models.⁷¹ Overall, AAMD is generally not used for simulating entire DNA origami devices. The computational cost of atomistic simulations often restricts their use to studying small DNA origami constructs (such as Seeman J1 sequences^{72,73}), subsections of DNA devices (where the rest of the DNA origami is fixed^{60,74,75}), or large structures for very short times.

Current force fields have shown great agreement with multiple experimental observations of DNA structure and dynamics, including sequence-dependent conformations, 77-80 deformability, 81,82 ionic conductivity, 83-85 spectroscopic features, 86-88 and DNA-surface interactions. 89,90 Force field refinement and creation will remain a process in constant evolution for as long as computer power continues improving and as the ever-growing access to longer time scales exposes the inaccuracies of existing force fields. We can thus expect additional uses of AAMD simulations to arise with the improvement of these models.

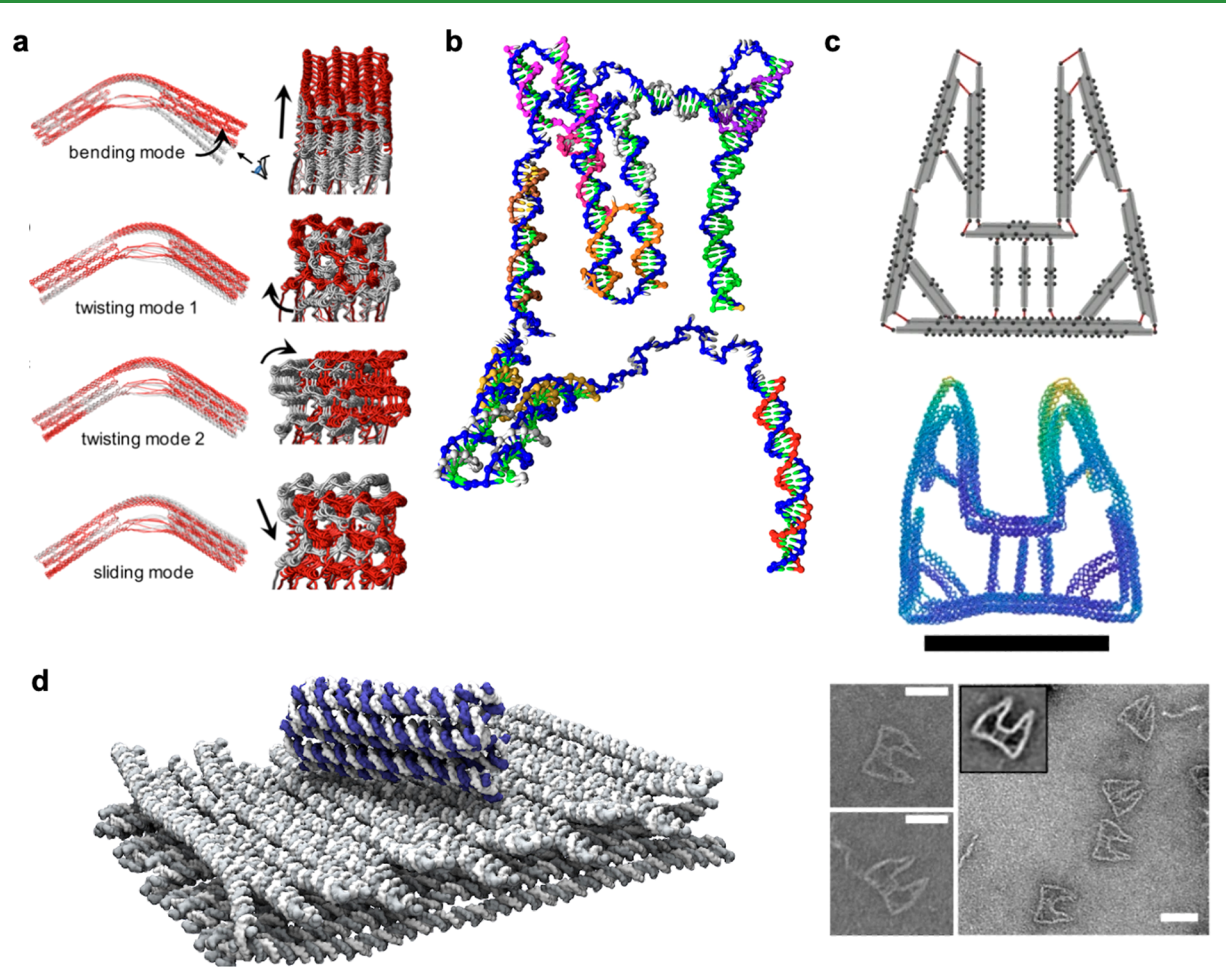


Figure 3. Coarse-grained modeling of DNA nanostructures. (a) Principal component analysis of a large DNA origami hinge. (b) Direct simulation of DNA nanostructure self-assembly. (c) Use of coarse-grained modeling as a predictor of the equilibrium shape of a nanopincer. (d) Characterization of a nanorotor made of DNA. (a) Reproduced with permission from ref 104. Copyright 2017 American Chemical Society. (b) Reproduced with permission from ref 105. Copyright 2016 American Chemical Society. (c) Reproduced with permission from ref 106. Copyright 2021 Springer Nature. (d) Reproduced with permission from ref 107. Copyright 2022 Elsevier.

Coarse-Grained Simulations. AAMD has two primary limitations when applied to simulations: hydrogen bonds have very fast vibrations, and so simulations conducted with timesteps beyond ~2 fs will encounter numerical instability and fail; and there may be many atoms in the system, resulting in expensive force calculations and a large amount of computation time for each increment of physical time being simulated. Coarse-grained (CG) representations and their corresponding CG molecular dynamics (CGMD) simulations attempt to circumvent both of these issues by changing the representation of molecules to one that is coarser than an atomistic representation. Coarse-grained modeling has been covered exhaustively in the past, 91 but we will provide a general overview here.

In this approach, groups of atoms are each considered as a single representative particle. This serves to remove fast vibrational modes from the system, which allows much larger timesteps to be used, and also reduces the quantity of particles in the system, which reduces the computational cost of force calculations at each time step. In addition, the many degrees of freedom arising from solvent molecules are removed by replacing the explicit solvent from AAMD with a simple implicit solvent representation. There are a few approaches to achieving such coarse graining. Some "top-down" schemes

attempt to reproduce experimentally characterized mechanical properties (e.g., bending and torsional persistence length and pitch of DNA) in addition to thermodynamic properties (e.g., melting temperature) through effective interaction potentials between coarse-grained particles. Other coarse graining techniques may begin with a reference AAMD simulation and attempt to match its equilibrium behaviors, which generally include distance and angle distributions between points in the AA model mapped to the CG particles. These "bottom-up" methods (readers are referred to multiple excellent reviews 93,94 on this topic) include iterative Boltzmann inversion (IBI), force matching, relative entropy minimization, and others. Machine learning approaches have also been used for bottom-up parametrization.

There have been a few different coarse-grained DNA models developed over the past decade, including Martini¹⁰⁰ and oxDNA, ¹⁰¹ among others. ^{102,103} The top-down parametrized oxDNA model has proven to be the most reliable at reproducing the behavior of large DNA nanostructures, and top-down models have generally provided better overall accuracy than bottom-up parametrizations. This is likely because top-down approaches focus on capturing specific characteristics of DNA, for example, propeller twist, major and minor groove spacing, and persistence length. All of these

characteristics are directly and intuitively related to the equilibrated structure, conformations, and other characteristics of DNA nanostructures that scientists desire to predict with simulations. However, bottom-up parametrization schemes often have a broad set of solutions, and many resulting potentials may be unphysical. For example, DNA can form a variety of structures, but AAMD simulations used for parametrization may only capture DNA as a duplex. Bottomup parametrization based on such simulations would thus not account for the myriad of other relevant DNA motifs such as Holliday junctions that are fundamental to DNA nanotechnology. Even if AAMD simulations used for parametrization did include whole DNA nanostructures with all possible motifs, bottom-up schemes with simple descriptions of potentials are not typically designed to handle the interaction complexity of DNA; therefore, the resulting model would be unlikely to correctly capture transitions or behaviors of other structures, or even the structure on which the parametrization was based. To summarize, top-down coarse-graining has provided the most accurate coarse-grained models because it focuses on directly reproducing features that are relevant to experimental observables.

Coarse graining's primary trade-off is the resulting loss of detail as compared to atomistic models; the particles are less well resolved, and the potentials have been fitted as an approximation to the interactions of many atoms, so they are not perfect and typically replace an anisotropic set of interactions (which may be functionally important) with a spherical or ellipsoidal approximation. In addition, solventspecific effects such as the aforementioned ionic effects are lost. However, the smallest modes of motion of AAMD simulations are typically not very important in the context of DNA nanotechnology, and many properties of interest can be reproduced using CG models. oxDNA has played a vital role in probing the equilibrium conformations of structures, stability verification of designs of large DNA nanostructures produced using common design packages, 108-115 structural characteristics of archetypal DNA origami structures, 116 conformations of ssDNA brushes on DNA origamis, 117 basic motion and reconfiguration of dynamic devices, 26,104,118–121 and DNA hybridization-based phenomena such as toehold-mediated strand displacement (TMSD). 92,122-124 The self-assembly of DNA nanostructures has even been directly simulated (Figure 3b). 105 Besides use in self-assembly, all of these examples used CG-based simulations to iteratively modify DNA nanostructure designs and ultimately control experimental outcomes without having to repeat experiments. It is further worth noting that this has become a somewhat standard practice that is not often reported in the literature; most DNA origami designs that have been fabricated for use in research were first simulated using CGMD and were often modified on the basis of results from these simulations.

Sometimes, instead of using MD simulations, Monte Carlo (MC) simulations ¹²⁵ can be used to sample the configurational space. This can be advantageous because this technique may offer larger physical jumps between sampled configurations resulting in more efficient sampling. MC simulations perform a sequence of perturbations of the particle configuration in a stochastic manner that is not associated with time integration and then accept or reject those moves based on the incurred energy change ΔE , typically according to the Metropolis acceptance criterion $P_{\rm acc} = \min(1, \exp(-\Delta E/k_{\rm B}T))$. This procedure enables thermodynamically valid sampling such that

the average of an observable in the simulation corresponds to the true ensemble average of that observable, which is ideally the expected value of that observable in an experiment. For dense systems such as DNA origami, MC move types that move a single particle tend to be inefficient. However, carefully constructed "cluster" move types that perturb groups of particles together may be drastically more efficient than MD. More complicated implementations of MC such as virtual move Monte Carlo (VMMC) enable these more sophisticated move types to be used¹⁰¹ and have been implemented in the oxDNA simulation package. Figure 3 presents a few representative examples where CG simulations have played a role in prediction and nanostructure design.

Mesoscopic Models. Along the same vein but perhaps deserving its own discussion, mesoscopic modeling (*meso* serving to describe an intermediate scale between molecular scale and macroscale systems) is an even coarser way to represent DNA structures. Generally, CG modeling groups a maximum of several atoms per representative particle and intends to use clusters of particles to mimic the behavior of monomers or small molecules; we can draw a distinction here for mesoscopic models, which further coarsen the representation of these systems to the point where the molecular detail is not well-defined.

Typically, representative particle size is on the order of a few nanometers or larger, and many mesoscopic models are beadchain models. At this scale, the molecular detail of the system is not of concern, and more emphasis is placed on reproducing properties that take place over larger length scales, for example, persistence length, end-to-end distance distributions, general shape of nanostructures, etc. This can be useful for capturing very coarse behaviors of dynamic nanostructures such as the opening and closing of hinges when several devices need to be considered simultaneously. This kind of simulation would be quite expensive to perform using finer models such as oxDNA but can be very efficiently performed using coarser representations. With such coarse models, the relaxation timecales of the particles often become shorter than the simulation time step so that the highly efficient overdamped Langevin dynamics (Brownian dynamics) simulations can be used to describe device motion. Mesoscopic models are also generally good candidates for implementation into lattice models. 126

While mesoscopic models have been used for studying various DNA-based systems such as chromatin, ^{127–133} DNA renaturation, ¹³⁴ DNA motion in microfluidic and nanofluidic systems, ^{135,136} and viral DNA packaging, ¹³⁷ they are generally underutilized in DNA nanotechnology. So far, mesoscopic models have been used in the beginning stages of multiscale models for modeling DNA nanostructures, ¹³⁸ and patchy mesoscopic representations of DNA building blocks have been used to elucidate the nucleated nature of DNA brick self-assembly ^{139,140} and the self-assembly of DNA tetrahedra into cubic diamond crystals. ¹⁴¹

Statistical Mechanics Models. Molecular simulation techniques are not generally capable of studying kinetic phenomena such as the folding of large DNA origami or the supramolecular assembly of larger structures from DNA origami tiles. Accessing the long time scales involved in these processes requires more efficient computational techniques or analytical treatments based on statistical mechanics. Statistical mechanics uses the statistical behavior of molecular systems (e.g., the Boltzmann relation at constant temperature)

to compute the long-time scale or bulk behavior of the system of interest. The ability to analyze systems using statistical mechanics comes from the observation that molecular microstates are Boltzmann distributed, $P_{\nu} \propto \exp(-\beta E_{\nu})$. Here, ν is a system microstate, E_{ν} is its energy, and $\beta \equiv 1/2$ $k_{\rm B}T$, where $k_{\rm B}$ is the Boltzmann constant and T is the system temperature. The partition function Q describes the sum of Boltzmann factors of all possible states in the system, or $Q = \sum_{\nu} e^{-\beta E_{\nu}}$ in the case of a constant T, constant number of particles, and constant volume (NVT) ensemble. The expectation value of any collective variable can thus be expressed as $\langle X \rangle = \sum_{\nu} X_{\nu} P_{\nu} = \sum_{\nu} X_{\nu} e^{-\beta E_{\nu}}/Q$. Statistical mechanics-based models developed for DNA origami applications to this date have generally addressed one of three objectives: prediction of the conformational dynamics and actuation behavior of dynamic DNA origami nanostructures, characterization of the dynamics of systems involving strand displacement reactions, and prediction of the kinetics and thermodynamics of assembly processes. Besides the general role of statistical mechanics in MD and MC simulations and in CG model development, 143 most existing methods have focused on fitting and predicting the behavior of simple dynamic DNA origami devices like hinges.²⁴ These systems usually incorporate short single-stranded molecules in each arm, referred to as "overhangs". The binding and unbinding of these overhangs, driven by actuation methods such as changes in salt concentration or TMSD, drives conformational changes between system states. Hybridization affinities are additionally controlled by tuning the length, sequence, and location of these strands. 120 The thermodynamic properties of the hinges are then fully described by hinge and overhang dynamics, whose effects can be decoupled. Marras et al.²⁶ and Crocker et al.¹⁴² used partition functions to characterize the free energy associated with ion- and temperature-mediated actuation of DNA origami nanohinges, respectively. These models have shown great agreement with experiments, suggesting notable control over the behavior of dynamic DNA origami nanodevices. However, their applications are limited to a narrow range of devices; theories and models characterizing the long-time behavior of dynamic DNA nanostructures are few and rare.

Kinetic Modeling. Many analysis techniques used in DNA computing and molecular programming, such as chemical reaction networks and automata-theoretic models, have diffused into structural and dynamic DNA nanotechnology, inspiring diverse mechanisms for actuation, communication, and programmability while providing fundamental insights into mechanistic processes such as those involving assembly. DNA origami platforms have been used to study the dynamic behavior of DNA strand displacement (DSD) systems, ensuring the (reaction-limited) spatial locality typical of other computing models. 144–146 While TMSD is often used for actuation, 12,24,147 in DSD systems, these reactions are used to execute signal processing and control instructions 146,148 such as logic gates, 44 fork and join gates, catalytic gates, neural network computation, 151 and oscillators. Integration of DNA and RNA enzyme strategies has expanded the design toolbox of these nucleic acid circuits, 153–155 allowing for the design of feedback control mechanisms, 156 predator—prey dynamics, 157 and transcriptional oscillators, 158 among other circuit implementations.

The system size that can be solved analytically 148 is limited and has long since been exceeded by the complexity of experimentally implemented circuits. Modeling techniques thus play an important role in determining the state space of DSD systems, ¹⁴⁸ estimating signal propagation times, ^{159,160} and verifying if the observed behavior of a system corresponds to the behavior predicted from design. 148 Two modeling approaches specifically stand out by virtue of their simplicity: reaction-diffusion equations and Brownian dynamics. 161 The kinetics of a DSD system can be modeled as a continuous time Markov process through the state space of all possible conformations, 159 which can be characterized either by means of mathematical treatments or stochastic simulations (i.e., Monte Carlo Gillespie algorithms). For simple DSD systems based strictly on strand displacement reactions, the different conformations of a system are defined by the state of the strands, and strand displacement reactions occur with an effective rate related to diffusion, hybridization-denaturation rates (typically modeled using specialized software such as Multistrand^{159'}), and the physical constraints of the system. These three properties can be integrated to obtain the effective strand displacement rates by means of reaction-diffusion equations, ¹⁴⁶, ¹⁶², ¹⁶⁶ or analytical theories involving first passage times. ¹⁶⁰ Most DSD analysis has now been automated and can be treated computationally using specialized kinetics software such as Visual DSD, 165 KinDA, 167 and DyNAMiC Workbench. 168

Similar modeling strategies have been used to design, program, and optimize the algorithmically directed assembly of DNA origami tiles. ^{169,170,187,188} A wide variety of DNA origami tile shapes and interactions are possible, ¹⁷¹ offering ways to build large, complex assemblies with nanoscale resolution. Experimentally implemented systems have been regulated by diverse physical processes, including hybridization, ¹⁷² strand displacement, ¹⁷³ shape complementarity, ^{171,174} and base stacking. ^{171,175} Knowledge of the thermodynamics and kinetics of tile binding can then be used as input for theoretical models at different levels of abstraction, including kinetic models, ^{170,176} Monte Carlo models, ¹⁷⁷ and chemical reaction networks. ^{178,179}

Kinetic modeling has also been used in structural and dynamic DNA nanotechnology systems beyond the context of DSD and tile systems. Many systems are purely reaction based, and so their behavior can be represented using mass-action kinetics, that is, as a system of ordinary differential equations (ODEs) describing the time evolution of concentration, which can be solved using eigenvalue decomposition or ODE solvers. To provide a few examples, kinetic modeling has been used to study individual attachment and detachment processes between separated DNA origami structures demonstrating autonomous regulation behavior, 180,181 and to describe the growth of polythymine brushes onto DNA via a catalytic enzymatic polymerization process.¹⁸² Strategies similar to those described for DSD systems have also been successfully implemented to model DNA origami folding. 183,185,186 Figure 4 depicts a few relevant kinetically modeled systems.

Continuum Modeling. While CGMD and mesoscale simulations are very useful in DNA nanotechnology and offer some of the best value in terms of accuracy versus computational cost, in some cases it is expedient to use continuum models. Continuum modeling assumes that the response of a system to a perturbation can be approximated as

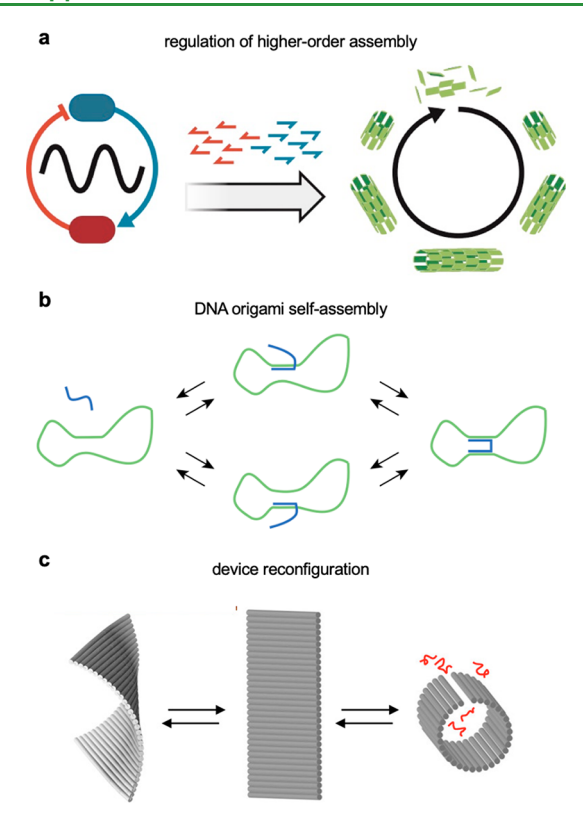


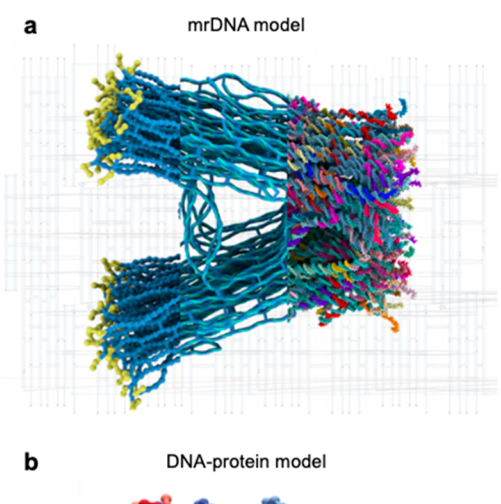
Figure 4. Kinetic modeling in DNA nanotechnology. (a) Kinetic model of higher-order self-assembly and disassembly of DNA nanotubes. (b) Kinetic model of DNA origami self-assembly. (c) Kinetic model of a reconfigurable DNA origami sheet. (a) Reproduced with permission from ref 180. Copyright 2019 Springer Nature. (b) Reproduced with permission from ref 183. Copyright 2015 AIP Publishing LLC. (c) Reproduced with permission from ref 184. Copyright 2014 American Chemical Society.

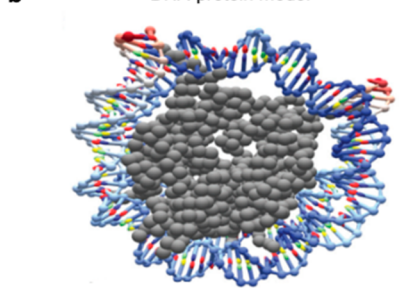
a continuous function satisfying macroscopic balance and conservation principles. When applied to solid mechanics, partial differential equations are often used to solve the spring equation for continuum solids to compute the global deformation response to an applied load, which is introduced as a boundary condition. When geometry is too complex to analytically solve this equation, the problem can be discretized into a set of small volumetric elements whose displacements are described by the equation f = Ku, where f is the set of all forces on connective elements (nodes), u is the displacement vector of the nodes, and K is a stiffness matrix that accounts for both compressive/tensile stiffness and bending and torsional stiffness within the element accounting for the intrinsic moduli of the material and moment of inertia of the element shape in the direction of the applied load. Continuity between all elements is assumed through their shared nodes, which converts this partial differential equation problem into a matrix algebra problem that can easily be solved.

A finite element model called CanDo¹⁸⁹ has been developed for continuum analysis of DNA nanostructures; this model treats individual nucleotides as connected continuum nonlinear beams (because DNA's behavior is more complex than the usual, linear macroscopic treatment of most isotropic engineering materials) and computes the equilibrium configuration and fluctuations of the DNA nanostructure being studied. While it does not serve as final validation for structural integrity or stability, CanDo is a good first check for having

attained the desired final structure before running a CG simulation, as CanDo can usually predict undesired twisting and bending of structures in a fraction of the simulation time required by CGMD simulations. This allows experimental groups designing DNA origami to quickly test their designs and return to the drawing board if significant undesired bending or twisting is predicted. The more recent SNUPI model 190 improves upon the CanDo model by adding electrostatic interactions and has been shown to work well for computing the equilibrium conformations of hierarchical superstructures consisting of many DNA origami, 191,192 a task that has proven quite challenging for both AAMD and CGMD simulations. Continuum mechanics provides additional value to DNA nanotechnology by providing practically useful quasianalytical scaling behavior of new systems. For example, basic solid mechanics including beam bending calculations based on moment of inertia can be used to intuitively explain the relationship between DNA origami cross section and structural persistence length with remarkable agreement. 193 This is useful because as DNA nanotechnology has been advancing in complexity (with nanostructures containing structural elements with many different cross sections being introduced recently 110), these continuum mechanics assumptions provide basic predictive power for controlling the deformation behavior of these structures and provide quantitative data for comparison of multiple cross sections when they, for example, contain the same overall cross-sectional area but different shapes.

Multiscale and Hybrid Resolution Models. There are some approaches that combine multiple modeling paradigms to address specific limitations of individual techniques. For example, some larger DNA nanostructures may be prohibitively expensive to equilibrate at a coarse-grained resolution. To address this, a model has been developed that performs major equilibration steps such as global structure relaxation at a mesoscopic resolution and gradually refines modeling resolution to achieve atomically reasonable equilibrium conformations in just a few minutes. 138 This model has the added benefit of accessing very long dynamic time scales for other purposes such as the simulation of applied electric fields. Other examples of hybrid approaches include a recently developed model that allows CGMD simulations of DNA to be run in the presence of a mesoscale protein representation 194 and, in the area of chromatin modeling, a mesoscale representation of DNA and a coarser representation of nucleosomes with charges represented using a discrete surface charge approach. ¹²⁸ Another multiscale model used oxDNA to sample the local free energy landscape of DNA brick selfassembly, and then used that data to produce a two-state kinetic rate model of the self-assembly process. 195 Examples of multiscale and hybrid resolution models can be found in Figure 5. Quantum Mechanics/Molecular Mechanics (QM/MM) multiscale models have also been used in limited context to study DNA. QM/MM models apply QM-based behavior to reactive species, for example, those undergoing some kind of chemical reaction, while treating other species using standard AAMD force fields within the same simulation. This enables time scale access approaching that of AAMD while still capturing the physics required for phenomena such as ATP hydrolysis 196 or enzyme activity. 197 In the context of DNA nanotechnology, combinations of QM and MD simulations have already been applied toward the optimization of dye placement⁷⁴ to afford control over device signal output and





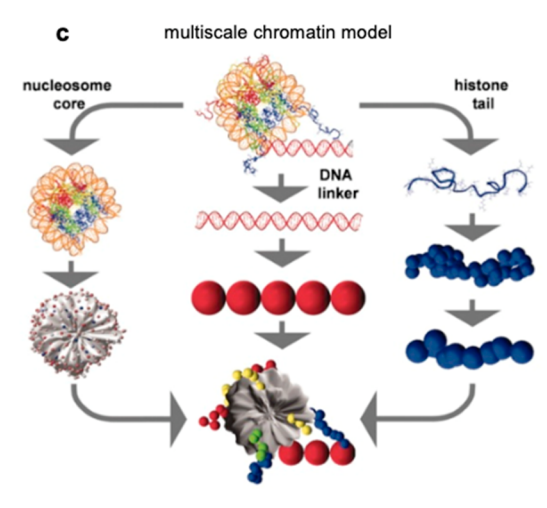


Figure 5. Three multiscale/hybrid scale models used to solve tractability problems in DNA nanotechnology. (a) Multiresolution DNA model used for rapid configurational equilibration. (b) Hybrid DNA—protein model for simulation of DNA and protein complexes. (c) Hybrid scale nucleosome—DNA model for simulation of chromatin. (a) Reproduced with permission from ref 138. Copyright 2020 Oxford University Press. (b) Reproduced with permission from ref 194. Copyright 2021 The Royal Society of Chemistry. (c) Reproduced with permission from ref 133. Copyright 2006 National Academy of Science.

could find future use in photonic systems 198 or systems containing quantum dots. $^{199-201}$

ANALYSIS OF SIMULATIONS

The objective of simulations is typically to produce data that can be compared to an experimental result or another simulation to provide interpretable information about system behavior. However, simply running simulations of DNA nanostructures and attempting to "observe" phenomena by eye is often insufficient to capture interesting phenomeno-

logical behavior. Trajectories must be analyzed to remove unimportant degrees of freedom and capture the true mean structure, dynamics, or some other property of the system. We will describe some of the most common analyses performed on simulations.

Mean Structure Computation and Removal of Diffusive Degrees of Freedom. Computation of the mean structure of a DNA nanodevice from dynamic simulations is often a first step in the process of trajectory analysis. Molecular simulations are often conducted on species that are floating in solution; these species correspondingly have six degrees of freedom (three degrees of translation and three axes of rotation), which are not relevant to the actual intradevice motion. To address this, we may isolate the specific components of the body of molecules that we want to analyze (excluding other bodies that do not participate in or are not relevant to the process under study) and perform a rotational and translational transform to minimize the mean squared distance between the selected particles in frame *i* and those particles in every other frame of the simulation. This frame i is often selected at random but may also be selected to force alignment to some basis, for example, Cartesian axes. This yields a trajectory of a structure that does not translate or rotate but instead solely performs its own internal motions, which is much easier to analyze. Taking the mean of this modified trajectory provides what is referred to as the "mean structure", which is the average structure accounting only for internal motions. Examples of where this analysis has been applied include characterizing polythymine brush extent on DNA nanostructures, ¹¹⁷ and capturing the mean structure of a dynamic DNA origami hinge, ¹²⁰ both of which demonstrated good agreement with experiments.

Principal Component Analysis. To determine the dynamical behavior of structures, one may conduct principal component analysis (PCA). 202 In a general sense, PCA generates a set of orthogonal vectors within a D-dimensional data set along which the first vector captures the largest deviation in that data set, the second vector captures the second largest deviation, and so forth, until there are no more orthogonal vectors that can be created. This results in D-1vectors or principal components. In the case of molecular simulations, PCA can be used to compute the combinations of particle motions that produce the largest overall deviation from the structure's mean. To do this, one can calculate the Cartesian displacement of particles in each frame from the mean structure of an N-particle system, flattening them into a vector of length 3N for each frame, computing a covariance matrix of this vector, and computing the eigenvectors and eigenvalues of that covariance matrix, where each eigenvector is a "component" of motion. These components can then be redistributed into a set of three-dimensional vectors v each accounting for the motion of a single particle. This is often diagrammatically represented using an image of the mean structure at c superimposed with a new image of the structure where each particle has been moved by its corresponding three-dimensional vector to locations $\mathbf{c} \pm \mathbf{v}$ (Figure 3a). With PCA, one can understand how a structure is moving, including determining whether undesired motions are occurring, thereby allowing researchers to better design dynamic devices to have more controlled motions. 104 The recent introduction of the oxView Web server²⁰³ enables these components to be computed easily.

ACS Applied Bio Materials

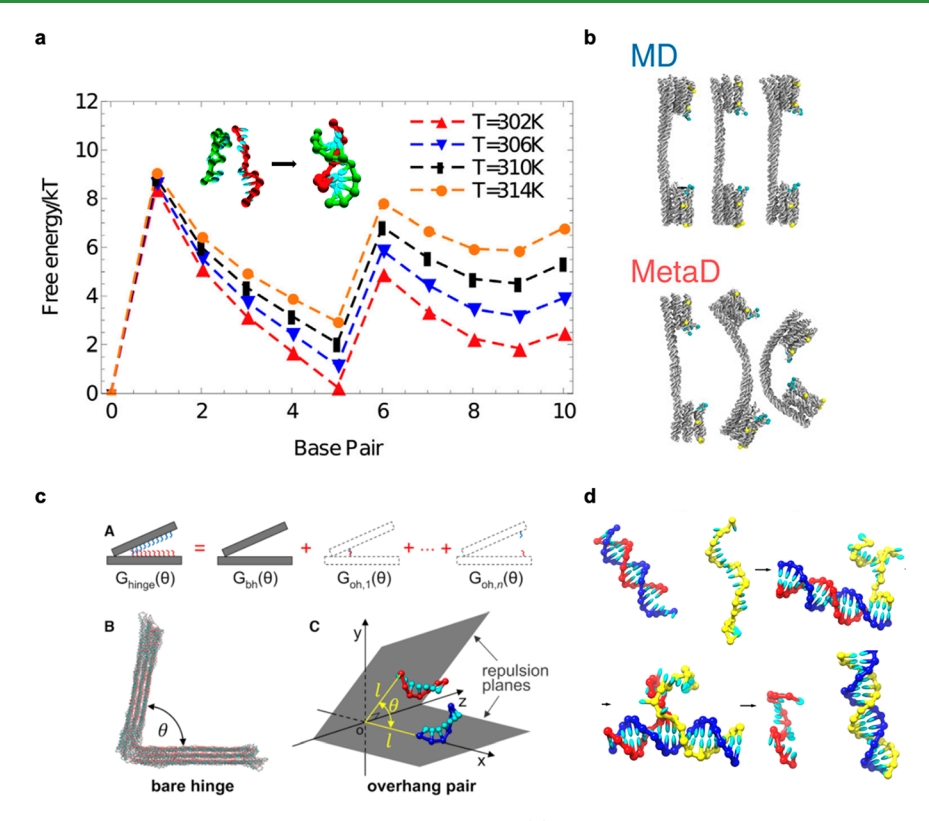


Figure 6. Use of enhanced sampling to predict DNA nanodevice behavior. (a) Pseudoknot formation in a dodecamer. (b) Metadynamics to improve conformational sampling of a DNA nanostructure. (c) Umbrella sampling using the hinge angle of a DNA nanostructure as a reaction coordinate. (d) Umbrella sampling of a toehold-mediated strand displacement reaction. (a) Adapted with permission from ref 101. Copyright 2021 Frontiers Media S.A. (b) Reproduced with permission from ref 209. Copyright 2022 American Chemical Society. (c) Reproduced with permission from ref 120. Copyright 2020 Oxford University Press. (d) Adapted with permission from ref 122. Copyright 2013 Oxford University Press.

ı

Estimating the Mechanical Properties of Structures.

The exact mechanical properties of DNA nanostructures could be of importance to future experiments in DNA nanotechnology. Past studies have focused on applying the principles of mechanical engineering beam analysis to DNA nanostructures. The chemistry and biophysics communities typically address the bending stiffness of DNA nanostructures in terms of persistence length l_p , whereas the mechanical engineering community tends to use quantities such as Young's modulus E and bending moment of inertia I to describe stiffness. These properties are connected by the relationship l_p = EI/k_BT . The persistence length can be computed using standard methods from MD simulations, 205 providing a quantity that can be compared against experiments. 206 The mechanical stiffness of other bodies such as hinges can be determined by calculating hinge angle distributions and computing the slope of the free energy landscape $dF/d\theta$.²⁴

Calculating Diffusion Coefficients. The diffusion of particles in a liquid, which is the typical environment for DNA systems, generally follows Stokes—Einstein behavior, 207 where the translational self-diffusivity D_s is inversely proportional to the particle's hydrodynamic radius. D_s can be ascertained in simulations from the slope of a plot of mean squared displacement as a function of time change t in the long-time limit. These diffusive statistics apply not only to a single isolated particle, but also to the centroid of a group of particles forming a single-stranded oligonucleotide or even an entire DNA origami, although many existing models such as oxDNA do not account for hydrodynamic interactions, 208 and so simulations using these may be inaccurate for comparison to

experimental techniques. AAMD simulations should hypothetically produce accurate diffusion behavior that accounts for hydrodynamics, although this technique suffers from periodic boundary condition artifacts and computational expense.

Enhanced Sampling and Computation of Energy **Landscapes.** The free energy of systems with respect to some reaction coordinate is often of interest. For example, one might wish to design a DNA hinge with a specific energy barrier to opening and closing. Describing such energy barriers and quantifying the time scale of transitions between states would likely involve conducting CGMD simulations of that hinge, which sample its full configurational space. However, such simulations might be prohibitively long because the transition time across barriers scales exponentially with barrier height normalized by thermal energy. For this reason, one can turn to enhanced sampling techniques such as umbrella sampling, metadynamics, or various other techniques.²¹⁰ Enhanced sampling applies a known bias to a simulation, which drives the system being studied out of local energy minima and then uses that bias to determine the free energy landscape along a reaction coordinate. Normally, the Hamiltonian of a system is simply a function of their coordinates \mathbf{r}^{N} and momenta \mathbf{p}^{N} : $H(\mathbf{r}^{N}\mathbf{p}^{N})$. As the most basic example, umbrella sampling modifies the Hamiltonian being used in the simulation to $H' = H(\mathbf{r}^N \mathbf{p}^N) + \frac{1}{2} k_{\chi} (\chi - \chi_0)^2$, where χ is the current location along the reaction coordinate being considered and χ_0 is some value around which we would like to sample, and k_{ν} is some stiffness that is selected roughly corresponding to how steep the energy gradient is along the area being sampled. By running simulations with this modified ("biased") Hamiltonian

for many different values of χ_0 such that there is a contiguous set of simulations with significant overlap in the distribution of χ between each, we can effectively force the sampling of the entire energy landscape of interest. These overlapping distributions in χ are then unbiased and combined using weighted histogram analysis²¹¹ to produce a contiguous free energy landscape across the entire range of χ . This is a simple yet very powerful paradigm, which has only recently begun to be exploited for more advanced analysis of DNA nanostructures. 104,120 Another enhanced sampling technique, metadynamics,²¹² defines a reaction coordinate and then begins sampling the energy landscape along that reaction coordinate. As sampling proceeds, artificial potentials (usually Gaussians) are added to the current location being sampled to favor exploring other sections of the energy landscape. This pushes the system out of well-sampled regions and into less wellsampled ones. Once the entire range of interest has been sampled, the artificial potentials are summed and inverted to reveal the true free energy landscape. This technique has been used to enhance the sampling of the configurational space of DNA nanostructures for comparison to experiments involving DNA origami with broad configurational flexibility, 209 but it has also been applied in a variety of biochemistry systems²¹³⁻²¹⁵ and will surely find additional uses. Figure 6 depicts a few studies utilizing enhanced sampling.

COMPARING SIMULATION RESULTS TO EXPERIMENTS

The value of predictive simulation data is somewhat limited unless a sufficiently large body of paired data, consisting of simulations and corroborative experimental data, has been produced to merit confidence that the simulations are accounting for all or nearly all sources of experimental variability. This experimental data may be generated in several ways, from direct imaging with light microscopy to fluorescence spectroscopy to more advanced and well-resolved techniques like cryo-electron microscopy (cryo-EM). Generally, simulations and experiments are compared by defining useful collective variables and then designing schemes for measuring those variables both in simulations and in experiments. The distributions or other features of these collective variables can then be compared between simulation and experiment to determine whether the model is capturing the relevant physics. We previously described the ways that simulations are processed to gather collective variables of interest; in this section, we will describe a few ways in which experiments are used to generate collective variable data that may be mappable to simulations.

Electrophoresis. The most common first step in experimental characterization of a DNA origami nanostructure is gel electrophoresis of the folding products. Because larger DNA species tend to flow more slowly through an agarose gel under an electric field, differently sized species will separate over time where they can be compared to reference DNA ladders. The separation of these species is based upon the general concept of electrophoretic terminal velocity ν . The net force F acting on a molecule carrying charge q and being driven by electric field E is given by $F = qE - \gamma \nu$, where γ is the friction coefficient of the species. Because agarose gel is highly viscous, species rapidly reach terminal velocity so F = 0 and thus $\nu = qE/\gamma$. Because q and γ scale differently with molecule size, larger DNA species tend to have a slower terminal velocity and thus migrate more slowly through the gel, resulting in a

band of DNA (identified using a loading dye) that is closer to the well where the sample was loaded than smaller species. For sufficiently long stimulation times, these DNA bands become so well separated that they can be distinguished from each other and individually isolated and further characterized. This technique is primarily comparative, as the ladder and existing known species serve as points of reference. However, this can be useful for identifying bulk aggregation, dimerization, disassembly, and other desired/undesired behavior. Furthermore, bands from these gels may be repurified and assayed directly to further characterize the experimental result. This may serve to corroborate modeling-based predictions of structural stability or instability, or to direct further modeling and simulation to understand the cause of experimental outcomes such as aggregation.

Direct Imaging. Atomic force microscopy (AFM) and transmission electron microscopy (TEM) are typically used to provide direct images of DNA nanostructures. AFM works on the principle of mechanical cantilever bending, where a nanoscale silicon cantilever with a sharp tip is dragged or tapped across a nanoscale surface; a laser beam pointed at the top of the cantilever helps to measure the cantilever's angular deflection, from which the height of the tip can be calculated. The height values z measured at each location x_iy scanned using a motorized stage then provide a three-dimensional map of surfaces at very high resolution. TEM works on the principle of an electron source, which fires electrons through a specimen and records the unscattered electron density behind the sample, providing an image of the specimen being sampled. This provides a massive amount of useful information that can be compared to simulations, ranging from simple qualitative comparison between images and equilibrium simulations 112 to measuring the extent of polymers grafted to DNA origami for comparison to CGMD simulations²¹⁶ or nanoparticles, ^{217,218} to measuring the angle distributions of hinge and lever nanodevices and comparing these distributions to simulations. 104 The complexity in this technique arises from measuring collective variables, which must generally be performed manually, although this can be enhanced using artificial intelligence (see below).

Spectroscopy. Spectroscopy is the study of matter's interactions with electromagnetic waves. This is often a coarse but very effective way of observing DNA nanostructures and their behavior. Within spectroscopy is fluorescence, a phenomenon where certain molecular species absorb light at one (often invisible) wavelength and then emit (usually visible) light in their excited state. The emitted light can be used to determine the locations of DNA nanostructure components that have been labeled with fluorescent groups. Fluorescent particle tracking has been used to characterize the free energy landscapes of DNA origami devices, revealing landscape features that are corroborated by CGMD simulations. 107 One adjacent example to fluorescence is Förster resonance energy transfer (FRET), a nonradiative dipole-dipole energy transfer phenomenon arising when one molecular species ("donor") is excited. If that species is close to a species that is capable of receiving energy from resonance energy transfer ("acceptor"), the excited donor species will shunt its energy to the acceptor species and excite it, then causing the acceptor to emit its characteristic excitation signal; if the donor is not close to an acceptor, the energy from excitation will be emitted as the donor's signal. When FRET pairs are placed on different parts of a DNA nanostructure, the

signal arising from that FRET pair can be used to determine whether those two parts are near each other or far away from each other. While very simple in nature, this is extremely useful as it can indicate open/closed states for hinge and box type structures² or can serve as a signal for whether a certain component has incorporated into or dissociated from a DNA nanostructure.²⁰ These data are also easy to corroborate with simulations because a simple collective variable can be defined on the basis of the separation of the pair's grafting locations and the system can be predicted using CGMD simulations.²¹⁹

Ultraviolet—visible (UV—vis) spectroscopy measures the absorption of UV and visible spectrum electromagnetic radiation by a sample. DNA's spectral absorption can be used to estimate the concentration of DNA in solution, ²²⁰ which can provide information about DNA nanostructure yield. The G-quadruplexes also have a distinct spectral absorbance from ssDNA or dsDNA, leading to the use of UV—vis spectroscopy to quantify the behavior of DNA-based nanoswitches. ²²¹ Finally, UV—vis spectroscopy has been used to quantify DNA binding onto gold nanoparticles. ²²²

As the characteristic energy levels of rotation and vibration of DNA molecules fall in the high gigahertz (GHz) to low terahertz (THz) spectra, ^{87,223-227} GHz to THz radiations these wavelengths have found use in manipulating DNA origami nanostructures, increasing their yield²²⁸ and allowing for the development of biosensors and antennas with tunable resonance. ²²⁹⁻²³¹ To better understand these devices, computational THz spectroscopy of DNA origami molecules can be performed using specialized software ^{86,232,233} and algorithms ^{234,235} together with atomistic simulations. ^{87,88} However, such treatment can only be implemented on small molecular systems.

Cryo-Electron Microscopy (Cryo-EM). Cryo-EM²³⁶ vitrifies samples at extremely low temperatures and then uses transmission electron microscopy (TEM) to resolve 2D projections of those samples. Mathematical transformations can be performed on the 2D data to recover 3D structural information.²³⁷ This can be used to resolve the structure or dynamics of proteins or DNA nanostructures in a nearly atomically precise manner. In DNA nanotechnology, cryo-EM reconstructions of DNA origami⁵² have been used as validation for new simulation models. ¹⁹⁰

Dynamic Light Scattering (DLS). DLS uses the autocorrelation of laser light scattering intensity to determine the diffusive properties of the species contained within a sample. It is most often used to obtain the diffusion coefficient of species and to estimate the hydrodynamic radius of those species. Por a single species in solution, the autocorrelation of scattering intensity decays as a single exponential with a decay constant $\tau = q^2$, where q is the wave vector and the translational self-diffusivity. This is relatively straightforward to compare to approximations for the diffusive properties of nonspherical shapes, Path 241 and 242 making for a useful point of comparison with the DLS result.

Small-Angle X-ray Scattering (SAXS). This technique is used to determine the sizes and distributions of nanoparticles in solution 239,244 in addition to their shapes and for distinguishing between different conformational states and resolving their transitions. SAXS functions on the same principle of standard X-ray scattering: when the paths of scattered X-rays differ by a perfect multiple of their wavelength λ , those X-rays collectively exhibit a high intensity from cooperativity, while paths differing by a perfect half multiple λ /

2 are mutually destructive and will produce essentially no scattered signal; SAXS data are typically a plot of scattering intensity as a function of scattering vector *q*; these data may be interpreted to provide information about particle size and shape, which can be compared directly to simulations. While its use has been limited, SAXS promises to resolve behavior similar to that captured using fluorescence, but without the use of bulky and saturation-prone fluorescent molecules.

Less Common Techniques. Some additional experimental characterization techniques applied toward DNA origami include small-angle neutron scattering, ²⁴⁶ ion mobility spectrometry—mass spectrometry, ²⁴⁷ and individual particle electron tomography. ²⁴⁸

ARTIFICIAL INTELLIGENCE AND MACHINE LEARNING

Artificial intelligence (AI) and machine learning (ML) are somewhat distinct from the rest of the methods covered in this Review because they are more general. However, due to the incredible power of inference, ML and AI have seen broad adoption across the domains of physics, 249,250 biology, 251,252 and materials science, 253,254 and discussion of their use in the context of prediction and control in DNA nanotechnology is warranted. AI is a discipline that concerns solving problems that cannot necessarily be addressed procedurally, in a manner inspired by the learning behaviors of intelligent beings such as humans. In most cases, AI attempts to establish a mapping relationship between some input and a desired output. This output may be, for example, the correct identification of the subject of an image or an estimation of the probability distribution of some collective variable. This process is often accomplished using feedback, 255-257 where the output is compared to the ground truth (expected outputs); the mapping function is then adjusted until it can reliably reproduce these input-output relationships.

As a subset of AI, ML covers algorithms capable of learning from pre-existing examples to make decisions or predictions by recognizing the underlying patterns of a problem. There are three main categories of ML: supervised learning, unsupervised learning, and reinforcement learning. Supervised learning is commonly adopted when a labeled data set is available for the model to capture the relationship between feature and label. However, unsupervised learning is adopted when labeling is physically or economically prohibited, or when the goal is to identify the underlying distribution of data, for example, using clustering algorithms. 258 Both supervised and unsupervised learning provide data-driven predictions on properties of interest. In the framework of reinforcement learning, the objective would be for an agent to identify an optimal strategy (policy) by maximizing a given reward function. The agent does this by directly interacting with the environment and learning from the received rewards. For how AI and ML techniques work, we refer readers to existing comprehensive literature addressing these topics. 259,260

In DNA nanotechnology, AI has been adopted to address emergent topics in the field, including nanostructure annotation, design optimization, and device development. The most straightforward application is to apply AI toward direct imaging data of DNA nanostructures. Correctly quantifying the values of collective variables in DNA nanostructures and annotating AFM imaging usually takes a tremendous amount of human input, where a researcher must manually label hundreds to thousands of data points to

establish sufficient statistical power in an experiment. AI promises to enable automated labeling of experimental data in a way that is not only less work but also less error-prone than manual human entry. ^{261–263} For example, YOLOv5 and its recent derivative YoloX, ²⁶⁴ convolutional neural networks that perform extraordinarily well in image recognition tasks, have been implemented in the context of nanostructure detection to avoid laborious manual annotation of AFM images, leading to a much more labor-efficient and statistically robust approach to distinguishing between DNA nanostructures²⁶⁵ and estimating their yields. A deep neural network has also been used to directly improve the resolution of DNA origami AFM images. 266 Similar goals can also be achieved by nano-TRON, 267 an open-source imaging package that performs classification tasks and has been shown to reliably reconstruct nanostructures from super-resolution DNA-PAINT²⁶⁸ imaging of DNA origami. A more recent study used AI to reduce the amount of sampling required to reconstruct these structures by an order of magnitude, ²⁶⁹ indicating that AI can be used to massively improve throughput in DNA nanotechnology-based imaging applications.

Beyond accelerating laborious analysis tasks, AI has also been applied to develop better DNA origami designs. In simulation work, researchers have implemented shape annealing and evolutionary strategies on the oxDNA model and simulation software package 10,92,270 to design nanostructures that closely match a desired shape profile.²⁷¹ AI has also been applied to provide a more accurate prediction of structural properties, for example, constructing quantumaccurate electron density profiles for DNA nanostructures up to ~225 kDa. 272 Another interesting experimental application of AI to DNA origami is the use of ML to predict and optimize the performance of molecular photonic wires based on their chromophore attachment configuration. 273 eXtreme Gradient Boosting (XGB)²⁷⁴ has additionally been used to classify the sequence of molecular barcodes for multiplexed detection of biomolecules on surfaces.2

■ GRAND CHALLENGES AND OPPORTUNITIES

The past decade has produced astounding advancements in our ability to understand and optimize the behavior of DNA nanodevices. However, several behaviors of DNA origami are still not under our control. First, the folding of DNA nanostructures and the associated yield of this process are not predictable. While several design and fabrication recipes help to avoid folding problems, 8,276,277 they must be developed on a case-by-case basis and do not always guarantee good folding results. Better understanding of the folding process will lead to much higher confidence that designs will fold properly, both within the field and when researchers adopt DNA origami as a tool in other fields.

Several properties of correctly assembled DNA nanostructures are also not very predictable, for example, the interaction of DNA with proteins. Addressing this issue is well underway, 194 but the field still lacks a coarse-grained force field capable of accurately capturing the interactions between different peptides and DNA. In addition to proteins, the effect of ions on DNA, specifically multivalent ions, may not be accurately captured with CG modeling. This is likely because CG models tend to treat salt effects using the Debye—Hückel theory, which is too simple to address multivalent ions. Currently, multivalent ion effects in the oxDNA model are treated by simply applying an artificially high monovalent ionic

concentration. While this treatment functions well in fabrication conditions, it is not clear how it will perform at multivalent ion conditions deviating significantly from those used during fabrication. This may potentially be resolved in the future using more complex CG interactions that account for other factors such as ion type, correlation, and valency in addition to ionic concentration. CG models in adjacent fields such as chromatin modeling have successfully reproduced multivalent cation-mediated effects, offering potential solutions to this challenge.

The size of the DNA nanostructures, especially those hierarchically assembled from multiple DNA origamis, is increasing at a rapid pace. At the larger length and time scales associated with these structures, existing CG simulation techniques are becoming insufficient to characterize dynamic behavior. Mesoscale models using a coarser representation than the oxDNA model may be useful for this purpose, where capturing transition behavior over micrometers and seconds may be tractable. The aforementioned mrDNA model may be a good starting framework for this.

Lastly, AI can be used to improve our understanding of several under-addressed topics in DNA nanotechnology. The first is to use AI to understand fundamental processes. For instance, one can exploit the inference power of ML models to predict the transition behavior of dynamic DNA origami devices. This can take place either in a simulation or in experiments for the inference of relevant collective variables, or in identifying interesting behavioral patterns. The second is to exploit AI to improve assembly yields and control defects. Instead of relying on expert intuition to craft assembly rules to obtain desired origami design with sufficient yields, we envision that reinforcement learning or active learning can be well suited for this type of task. The third is to encourage the use of AI in DNA technology by improving data accessibility. Powerful ML models have achieved great success in other research fields, such as Alphafold 2²⁷⁹ in the protein field, largely thanks to the existence of vast data repositories such as the RCSB Protein Data Bank.²⁸⁰ Yet, the adoption of ML has been relatively slow in DNA nanotechnology because there has not historically been a database or a data-sharing platform for DNA nanostructure data, hindering AI workers from accessing data and extracting knowledge or building models on it. A promising new resource in the DNA nanotechnology space has been Nanobase, a database and repository for DNA nanostructures.²⁸¹ This makes it possible to see the designs used in various publications in the field, with additional data available describing fabrication protocols. This resource could be further leveraged in AI and ML applications and in data harvesting for the enhancement of the field if additional information about these nanostructures was provided, for example, AFM or TEM images of folding products and standardized and accessible data fields for annealing ramps and salt conditions used in the fabrication of these nanostructures. This could potentially aid in the improvement of our understanding of DNA origami folding and provide a robust body of reference data against which new simulation models may be parametrized. Another way that ML and especially deep learning can contribute is in the development of simulation force fields where AI can provide nonfunctional parametrization of CG force fields that may be more accurate than functional representations.

CONCLUSION

In this Review, we discussed the broad range of time and length scales over which events in DNA nanotechnology take place and the modeling resolutions used to represent DNA nanostructures at these length and time scales. We then discussed different simulation methods for the prediction and control of DNA structure and device behavior. We described the different experimental characterization techniques that are available for comparison to model predictions and how they are used in synergy with modeling for practical device design and fabrication. We then discussed the recent development of AI- and ML-based tools for DNA nanotechnology. Finally, we discussed the current limitations and gaps in the modeling and simulation space and identified key opportunities in prediction and control that may further aid in the advancement of the field.

AUTHOR INFORMATION

Corresponding Author

Gaurav Arya — Thomas Lord Department of Mechanical Engineering and Materials Science, Duke University, Durham, North Carolina 27708, United States; orcid.org/0000-0002-5615-0521; Email: gaurav.arya@duke.edu

Authors

Marcello DeLuca — Thomas Lord Department of Mechanical Engineering and Materials Science, Duke University, Durham, North Carolina 27708, United States; ◎ orcid.org/0000-0002-4299-3501

Sebastian Sensale – Department of Physics, Cleveland State University, Cleveland, Ohio 44115, United States

Po-An Lin — Thomas Lord Department of Mechanical Engineering and Materials Science, Duke University, Durham, North Carolina 27708, United States

Complete contact information is available at: https://pubs.acs.org/10.1021/acsabm.2c01045

Notes

The authors declare no competing financial interest.

ACKNOWLEDGMENTS

This work is supported by the National Science Foundation (Grant nos. CMMI-1921955 and EFMA-1933344) and the U.S. Department of Energy (Grant no. DE-SC0020996). M.D. is supported by the National Science Foundation Graduate Research Fellowship (Grant no. DGE-2139754). P.-A.L. is supported by the Duke University AI for Understanding and Designing Materials (aiM) Graduate Training Program funded by the National Science Foundation (Grant no. DGE-2022040).

■ REFERENCES

- (1) Seeman, N. C. Nucleic acid junctions and lattices. *J. Theor. Biol.* **1982**, 99 (2), 237–47.
- (2) Selnihhin, D.; Sparvath, S. M.; Preus, S.; Birkedal, V.; Andersen, E. S. Multifluorophore DNA origami beacon as a biosensing platform. *ACS Nano* **2018**, *12* (6), 5699–5708.
- (3) Zhang, Q.; Jiang, Q.; Li, N.; Dai, L.; Liu, Q.; Song, L.; Wang, J.; Li, Y.; Tian, J.; Ding, B. DNA origami as an in vivo drug delivery vehicle for cancer therapy. ACS Nano 2014, 8 (7), 6633–6643.
- (4) Hudoba, M. W.; Luo, Y.; Zacharias, A.; Poirier, M. G.; Castro, C. E. Dynamic DNA origami device for measuring compressive depletion forces. *ACS Nano* **2017**, *11* (7), 6566–6573.

- (5) Liu, H.; Wang, J.; Song, S.; Fan, C.; Gothelf, K. V. A DNA-based system for selecting and displaying the combined result of two input variables. *Nat. Commun.* **2015**, 6 (1), 1-7.
- (6) Kuzyk, A.; Schreiber, R.; Fan, Z.; Pardatscher, G.; Roller, E.-M.; Högele, A.; Simmel, F. C.; Govorov, A. O.; Liedl, T. DNA-based self-assembly of chiral plasmonic nanostructures with tailored optical response. *Nature* **2012**, *483* (7389), 311–314.
- (7) Shen, J.; Sun, W.; Liu, D.; Schaus, T.; Yin, P. Three-dimensional nanolithography guided by DNA modular epitaxy. *Nat. Mater.* **2021**, 20 (5), 683–690.
- (8) Rothemund, P. W. Folding DNA to create nanoscale shapes and patterns. *Nature* **2006**, 440 (7082), 297–302.
- (9) Ouldridge, T. E.; Louis, A. A.; Doye, J. P. Structural, mechanical, and thermodynamic properties of a coarse-grained DNA model. *J. Chem. Phys.* **2011**, *134* (8), No. 085101.
- (10) Sulc, P.; Romano, F.; Ouldridge, T. E.; Rovigatti, L.; Doye, J. P.; Louis, A. A. Sequence-dependent thermodynamics of a coarse-grained DNA model. *J. Chem. Phys.* **2012**, *137* (13), 135101.
- (11) Bustamante, C.; Bryant, Z.; Smith, S. B. Ten years of tension: single-molecule DNA mechanics. *Nature* **2003**, 421 (6921), 423–427.
- (12) Yurke, B.; Turberfield, A. J.; Mills, A. P.; Simmel, F. C.; Neumann, J. L. A DNA-fuelled molecular machine made of DNA. *Nature* **2000**, *406* (6796), 605–608.
- (13) Krzyźaniak, A.; Salański, P.; Jurczak, J.; Barciszewski, J. B–Z DNA reversible conformation changes effected by high pressure. *FEBS letters* **1991**, 279 (1), 1–4.
- (14) Mao, C.; Sun, W.; Shen, Z.; Seeman, N. C. A nanomechanical device based on the B–Z transition of DNA. *Nature* **1999**, 397 (6715), 144–146.
- (15) Ussery, D. W. DNA Structure: A-, B-and Z-DNA Helix Families. *Encyclopedia of life sciences* **2002**, 1–7.
- (16) Praetorius, F.; Kick, B.; Behler, K. L.; Honemann, M. N.; Weuster-Botz, D.; Dietz, H. Biotechnological mass production of DNA origami. *Nature* **2017**, *552* (7683), 84–87.
- (17) Lucas, C. R.; Halley, P. D.; Chowdury, A. A.; Harrington, B. K.; Beaver, L.; Lapalombella, R.; Johnson, A. J.; Hertlein, E. K.; Phelps, M. A.; Byrd, J. C. DNA Origami Nanostructures Elicit Dose-Dependent Immunogenicity and Are Nontoxic up to High Doses In Vivo. *Small* **2022**, *18*, 2108063.
- (18) Gyarfas, B.; Abu-Shumays, R.; Wang, H.; Dunbar, W. B. Measuring single-molecule DNA hybridization by active control of DNA in a nanopore. *Biophysical journal* **2011**, *100* (6), 1509–1516.
- (19) Xu, S.; Zhan, J.; Man, B.; Jiang, S.; Yue, W.; Gao, S.; Guo, C.; Liu, H.; Li, Z.; Wang, J. Real-time reliable determination of binding kinetics of DNA hybridization using a multi-channel graphene biosensor. *Nat. Commun.* **2017**, *8* (1), 1–10.
- (20) Schneider, F.; Möritz, N.; Dietz, H. The sequence of events during folding of a DNA origami. *Science advances* **2019**, 5 (5), eaaw1412.
- (21) Wagenbauer, K. F.; Sigl, C.; Dietz, H. Gigadalton-scale shape-programmable DNA assemblies. *Nature* **2017**, *552* (7683), 78–83.
- (22) Wang, Y.; Dai, L.; Ding, Z.; Ji, M.; Liu, J.; Xing, H.; Liu, X.; Ke, Y.; Fan, C.; Wang, P. DNA origami single crystals with Wulff shapes. *Nat. Commun.* 2021, 12 (1), 1–8.
- (23) Zhang, T.; Hartl, C.; Frank, K.; Heuer-Jungemann, A.; Fischer, S.; Nickels, P. C.; Nickel, B.; Liedl, T. 3D DNA origami crystals. *Adv. Mater.* **2018**, *30* (28), 1800273.
- (24) Marras, A. E.; Zhou, L.; Su, H.-J.; Castro, C. E. Programmable motion of DNA origami mechanisms. *Proc. Natl. Acad. Sci. U. S. A.* **2015**, *112* (3), 713–718.
- (25) Gerling, T.; Wagenbauer, K. F.; Neuner, A. M.; Dietz, H. Dynamic DNA devices and assemblies formed by shape-complementary, non-base pairing 3D components. *Science* **2015**, 347 (6229), 1446–1452.
- (26) Marras, A. E.; Shi, Z.; Lindell, M. G., III; Patton, R. A.; Huang, C.-M.; Zhou, L.; Su, H.-J.; Arya, G.; Castro, C. E. Cation-activated avidity for rapid reconfiguration of DNA nanodevices. *ACS Nano* **2018**, *12* (9), 9484–9494.

- (27) Kohn, W.; Becke, A. D.; Parr, R. G. Density functional theory of electronic structure. *J. Phys. Chem.* **1996**, *100* (31), 12974–12980.
- (28) Car, R.; Parrinello, M. Unified approach for molecular dynamics and density-functional theory. *Physical review letters* **1985**, 55 (22), 2471.
- (29) Wang, H.; Lewis, J. P.; Sankey, O. F. Band-gap tunneling states in DNA. *Physical review letters* **2004**, 93 (1), No. 016401.
- (30) Priyadarshy, S.; Risser, S.; Beratan, D. DNA is not a molecular wire: protein-like electron-transfer predicted for an extended π -electron system. *J. Phys. Chem.* **1996**, 100 (44), 17678–17682.
- (31) Beratan, D. N. Why are DNA and protein electron transfer so different. *Annu. Rev. Phys. Chem.* **2019**, 70 (1), 71–97.
- (32) Porath, D.; Lapidot, N.; Gomez-Herrero, J. Charge transport in DNA-based devices. *Introducing Molecular Electronics*; Springer: New York, 2006; pp 411–444.
- (33) Lech, C. J.; Heddi, B.; Phan, A. T. Guanine base stacking in G-quadruplex nucleic acids. *Nucleic acids research* **2013**, *41* (3), 2034–2046.
- (34) Gkionis, K.; Kruse, H.; Platts, J. A.; Mladek, A.; Koca, J.; Sponer, J. Ion binding to quadruplex DNA stems. Comparison of MM and QM descriptions reveals sizable polarization effects not included in contemporary simulations. *J. Chem. Theory Comput.* **2014**, *10* (3), 1326–1340.
- (35) Li, X.-Z.; Walker, B.; Michaelides, A. Quantum nature of the hydrogen bond. *Proc. Natl. Acad. Sci. U. S. A.* **2011**, *108* (16), 6369–6373.
- (36) Parker, T. M.; Hohenstein, E. G.; Parrish, R. M.; Hud, N. V.; Sherrill, C. D. Quantum-mechanical analysis of the energetic contributions to π stacking in nucleic acids versus rise, twist, and slide. *J. Am. Chem. Soc.* **2013**, *135* (4), 1306–1316.
- (37) Šponer, J.; Sabat, M.; Gorb, L.; Leszczynski, J.; Lippert, B.; Hobza, P. The effect of metal binding to the N7 site of purine nucleotides on their structure, energy, and involvement in base pairing. *J. Phys. Chem. B* **2000**, *104* (31), 7535–7544.
- (38) Jorgensen, W. L.; Maxwell, D. S.; Tirado-Rives, J. Development and testing of the OPLS all-atom force field on conformational energetics and properties of organic liquids. *J. Am. Chem. Soc.* **1996**, 118 (45), 11225–11236.
- (39) Ma, H.; Govoni, M.; Galli, G. Quantum simulations of materials on near-term quantum computers. *npj Computational Materials* **2020**, *6* (1), 1–8.
- (40) McCammon, J. A.; Gelin, B. R.; Karplus, M. Dynamics of folded proteins. *nature* 1977, 267 (5612), 585-590.
- (41) Levitt, M. Computer Simulation of DNA Double-Helix Dynamics; Cold Spring Harbor Symposia on Quantitative Biology; Cold Spring Harbor Laboratory Press: Plainview, NY, 1983; pp 251–262.
- (42) Tidor, B.; Irikura, K. K.; Brooks, B. R.; Karplus, M. Dynamics of DNA oligomers. *J. Biomol. Struct. Dyn.* **1983**, *1* (1), 231–252.
- (43) Beveridge, D. L.; Cheatham, T. E.; Mezei, M. The ABCs of molecular dynamics simulations on B-DNA, circa 2012. *Journal of biosciences* **2012**, *37* (3), 379–397.
- (44) Cornell, W. D.; Cieplak, P.; Bayly, C. I.; Gould, I. R.; Merz, K. M.; Ferguson, D. M.; Spellmeyer, D. C.; Fox, T.; Caldwell, J. W.; Kollman, P. A. A second generation force field for the simulation of proteins, nucleic acids, and organic molecules. *J. Am. Chem. Soc.* **1995**, 117 (19), 5179–5197.
- (45) MacKerell, A. D., Jr; Banavali, N.; Foloppe, N. Development and current status of the CHARMM force field for nucleic acids. *Biopolymers: original Research on biomolecules* **2000**, *56* (4), 257–265.
- (46) Zhu, X.; Lopes, P. E.; MacKerell, A. D., Jr Recent developments and applications of the CHARMM force fields. Wiley Interdisciplinary Reviews: Computational Molecular Science 2012, 2 (1), 167–185.
- (47) McConnell, K.; Nirmala, R.; Young, M.; Ravishanker, G.; Beveridge, D. A nanosecond molecular dynamics trajectory for a B DNA double helix: evidence for substates. *J. Am. Chem. Soc.* **1994**, *116* (10), 4461–4462.
- (48) Cheatham, T. I.; Miller, J.; Fox, T.; Darden, T.; Kollman, P. Molecular dynamics simulations on solvated biomolecular systems:

- the particle mesh Ewald method leads to stable trajectories of DNA, RNA, and proteins. J. Am. Chem. Soc. 1995, 117 (14), 4193-4194.
- (49) Kim, S. Issues on the choice of a proper time step in molecular dynamics. *Physics Procedia* **2014**, *53*, 60–62.
- (50) Doye, J. P.; Ouldridge, T. E.; Louis, A. A.; Romano, F.; Šulc, P.; Matek, C.; Snodin, B. E.; Rovigatti, L.; Schreck, J. S.; Harrison, R. M. Coarse-graining DNA for simulations of DNA nanotechnology. *Phys. Chem. Chem. Phys.* **2013**, *15* (47), 20395–20414.
- (51) Shaw, D. E.; Grossman, J.; Bank, J. A.; Batson, B.; Butts, J. A.; Chao, J. C.; Deneroff, M. M.; Dror, R. O.; Even, A.; Fenton, C. H. Anton 2: Raising the bar for performance and programmability in a special-purpose molecular dynamics supercomputer. SC'14: Proceedings of the International Conference for High Performance Computing, Networking, Storage and Analysis; IEEE: New York, 2014; pp 41–53.
- (52) Maffeo, C.; Yoo, J.; Aksimentiev, A. De novo reconstruction of DNA origami structures through atomistic molecular dynamics simulation. *Nucleic acids research* **2016**, 44 (7), 3013–3019.
- (53) Yoo, J.; Winogradoff, D.; Aksimentiev, A. Molecular dynamics simulations of DNA–DNA and DNA–protein interactions. *Curr. Opin. Struct. Biol.* **2020**, *64*, 88–96.
- (54) Yoo, J.; Aksimentiev, A. In situ structure and dynamics of DNA origami determined through molecular dynamics simulations. *Proc. Natl. Acad. Sci. U. S. A.* **2013**, *110* (50), 20099–20104.
- (55) Lavery, R.; Zakrzewska, K.; Beveridge, D.; Bishop, T. C.; Case, D. A.; Cheatham, T., III; Dixit, S.; Jayaram, B.; Lankas, F.; Laughton, C. A systematic molecular dynamics study of nearest-neighbor effects on base pair and base pair step conformations and fluctuations in B-DNA. *Nucleic acids research* **2010**, 38 (1), 299–313.
- (56) Pajak, J.; Dill, E.; Reyes-Aldrete, E.; White, M. A.; Kelch, B. A.; Jardine, P. J.; Arya, G.; Morais, M. C. Atomistic basis of force generation, translocation, and coordination in a viral genome packaging motor. *Nucleic acids research* **2021**, 49 (11), 6474–6488.
- (57) Ohmann, A.; Li, C.-Y.; Maffeo, C.; Al Nahas, K.; Baumann, K. N.; Göpfrich, K.; Yoo, J.; Keyser, U. F.; Aksimentiev, A. A synthetic enzyme built from DNA flips 107 lipids per second in biological membranes. *Nat. Commun.* **2018**, *9* (1), 1–9.
- (58) Bai, X.-c.; Martin, T. G.; Scheres, S. H.; Dietz, H. Cryo-EM structure of a 3D DNA-origami object. *Proc. Natl. Acad. Sci. U. S. A.* **2012**, *109* (49), 20012–20017.
- (59) Klaus, M.; Prokoph, N.; Girbig, M.; Wang, X.; Huang, Y.-H.; Srivastava, Y.; Hou, L.; Narasimhan, K.; Kolatkar, P. R.; Francois, M. Structure and decoy-mediated inhibition of the SOX18/Prox1-DNA interaction. *Nucleic acids research* **2016**, *44* (8), 3922–3935.
- (60) Ottaviani, A.; Iacovelli, F.; Idili, A.; Falconi, M.; Ricci, F.; Desideri, A. Engineering a responsive DNA triple helix into an octahedral DNA nanostructure for a reversible opening/closing switching mechanism: a computational and experimental integrated study. *Nucleic acids research* **2018**, 46 (19), 9951–9959.
- (61) Li, C.-Y.; Hemmig, E. A.; Kong, J.; Yoo, J.; Hernández-Ainsa, S.; Keyser, U. F.; Aksimentiev, A. Ionic conductivity, structural deformation, and programmable anisotropy of DNA origami in electric field. *ACS Nano* **2015**, *9* (2), 1420–1433.
- (62) Slone, S. M.; Li, C.-Y.; Yoo, J.; Aksimentiev, A. Molecular mechanics of DNA bricks: in situ structure, mechanical properties and ionic conductivity. *New J. Phys.* **2016**, *18* (5), No. 055012.
- (63) Roodhuizen, J. A.; Hendrikx, P. J.; Hilbers, P. A.; de Greef, T. F.; Markvoort, A. J. Counterion-dependent mechanisms of DNA origami nanostructure stabilization revealed by atomistic molecular simulation. *ACS Nano* **2019**, *13* (9), 10798–10809.
- (64) Yoo, J.; Aksimentiev, A. Molecular Dynamics of Membrane-Spanning DNA Channels: Conductance Mechanism, Electro-Osmotic Transport, and Mechanical Gating. *J. Phys. Chem. Lett.* **2015**, *6* (23), 4680–7
- (65) Göpfrich, K.; Li, C.-Y.; Mames, I.; Bhamidimarri, S. P.; Ricci, M.; Yoo, J.; Mames, A.; Ohmann, A.; Winterhalter, M.; Stulz, E. Ion channels made from a single membrane-spanning DNA duplex. *Nano Lett.* **2016**, *16* (7), 4665–4669.
- (66) Göpfrich, K.; Li, C.-Y.; Ricci, M.; Bhamidimarri, S. P.; Yoo, J.; Gyenes, B.; Ohmann, A.; Winterhalter, M.; Aksimentiev, A.; Keyser,

- U. F. Large-conductance transmembrane porin made from DNA origami. ACS Nano 2016, 10 (9), 8207-8214.
- (67) Maingi, V.; Lelimousin, M.; Howorka, S.; Sansom, M. S. Gating-like motions and wall porosity in a DNA nanopore scaffold revealed by molecular simulations. *ACS Nano* **2015**, *9* (11), 11209–11217.
- (68) Maingi, V.; Burns, J. R.; Uusitalo, J. J.; Howorka, S.; Marrink, S. J.; Sansom, M. S. Stability and dynamics of membrane-spanning DNA nanopores. *Nat. Commun.* **2017**, *8* (1), 1–12.
- (69) Yoo, J.; Aksimentiev, A. Competitive binding of cations to duplex DNA revealed through molecular dynamics simulations. *J. Phys. Chem. B* **2012**, *116* (43), 12946–12954.
- (70) Kastenholz, M. A.; Schwartz, T. U.; Hünenberger, P. H. The transition between the B and Z conformations of DNA investigated by targeted molecular dynamics simulations with explicit solvation. *Biophysical journal* **2006**, *91* (8), 2976–2990.
- (71) Chakraborty, S.; Sharma, S.; Maiti, P. K.; Krishnan, Y. The poly dA helix: a new structural motif for high performance DNA-based molecular switches. *Nucleic acids research* **2009**, *37* (9), 2810–2817.
- (72) Adendorff, M. R.; Tang, G. Q.; Millar, D. P.; Bathe, M.; Bricker, W. P. Computational investigation of the impact of core sequence on immobile DNA four-way junction structure and dynamics. *Nucleic acids research* **2022**, *50* (2), 717–730.
- (73) Hanke, M.; Dornbusch, D.; Hadlich, C.; Rossberg, A.; Hansen, N.; Grundmeier, G.; Tsushima, S.; Keller, A.; Fahmy, K. Anion-specific structure and stability of guanidinium-bound DNA origami. *Computational and Structural Biotechnology Journal* **2022**, *20*, 2611.
- (74) Cervantes-Salguero, K.; Biaggne, A.; Youngsman, J. M.; Ward, B. M.; Kim, Y. C.; Li, L.; Hall, J. A.; Knowlton, W. B.; Graugnard, E.; Kuang, W. Strategies for controlling the spatial orientation of single molecules tethered on DNA origami templates physisorbed on glass substrates: Intercalation and stretching. *International journal of molecular sciences* 2022, 23 (14), 7690.
- (75) Mathur, D.; Kim, Y. C.; Díaz, S. n. A.; Cunningham, P. D.; Rolczynski, B. S.; Ancona, M. G.; Medintz, I. L.; Melinger, J. S. Can a DNA origami structure constrain the position and orientation of an attached dye molecule? *J. Phys. Chem. C* 2021, 125 (2), 1509–1522.
- (76) Khosravi, R.; Ghasemi, R. H.; Soheilifard, R. Design and simulation of a DNA origami nanopore for large cargoes. *Molecular Biotechnology* **2020**, *62* (9), 423–432.
- (77) Pérez, A.; Blas, J. R.; Rueda, M.; López-Bes, J. M.; de la Cruz, X.; Orozco, M. Exploring the essential dynamics of B-DNA. *J. Chem. Theory Comput.* **2005**, *1* (5), 790–800.
- (78) Dans, P. D.; Perez, A.; Faustino, I.; Lavery, R.; Orozco, M. Exploring polymorphisms in B-DNA helical conformations. *Nucleic acids research* **2012**, 40 (21), 10668–10678.
- (79) Pasi, M.; Maddocks, J. H.; Beveridge, D.; Bishop, T. C.; Case, D. A.; Cheatham, T., III; Dans, P. D.; Jayaram, B.; Lankas, F.; Laughton, C. μ ABC: a systematic microsecond molecular dynamics study of tetranucleotide sequence effects in B-DNA. *Nucleic acids research* **2014**, 42 (19), 12272–12283.
- (80) Dixit, S. B.; Beveridge, D. L.; Case, D. A.; Cheatham, T. E., 3rd; Giudice, E.; Lankas, F.; Lavery, R.; Maddocks, J. H.; Osman, R.; Sklenar, H. Molecular dynamics simulations of the 136 unique tetranucleotide sequences of DNA oligonucleotides. II: sequence context effects on the dynamical structures of the 10 unique dinucleotide steps. *Biophysical journal* **2005**, *89* (6), 3721–3740.
- (81) Olson, W. K.; Gorin, A. A.; Lu, X.-J.; Hock, L. M.; Zhurkin, V. B. DNA sequence-dependent deformability deduced from protein—DNA crystal complexes. *Proc. Natl. Acad. Sci. U. S. A.* **1998**, 95 (19), 11163–11168.
- (82) Lankaš, F.; Šponer, J.; Langowski, J.; Cheatham, T. E., III DNA basepair step deformability inferred from molecular dynamics simulations. *Biophysical journal* **2003**, *85* (5), 2872–2883.
- (83) Aksimentiev, A.; Schulten, K. Imaging α -hemolysin with molecular dynamics: ionic conductance, osmotic permeability, and the electrostatic potential map. *Biophysical journal* **2005**, 88 (6), 3745–3761.

- (84) Aksimentiev, A.; Heng, J. B.; Timp, G.; Schulten, K. Microscopic kinetics of DNA translocation through synthetic nanopores. *Biophysical journal* **2004**, *87* (3), 2086–2097.
- (85) Sensale, S.; Peng, Z.; Chang, H.-C. Biphasic signals during nanopore translocation of DNA and nanoparticles due to strong ion cloud deformation. *Nanoscale* **2019**, *11* (47), 22772–22779.
- (86) Wang, F.; Zhao, D.; Dong, H.; Jiang, L.; Huang, L.; Liu, Y.; Li, S. THz spectra and corresponding vibrational modes of DNA base pair cocrystals and polynucleotides. *Spectrochimica Acta Part A: Molecular and Biomolecular Spectroscopy* **2018**, 200, 195–201.
- (87) Sensale, S.; Peng, Z.; Chang, H.-C. Kinetic theory for DNA melting with vibrational entropy. *J. Chem. Phys.* **2017**, *147* (13), 135101.
- (88) Wu, K.; Qi, C.; Zhu, Z.; Wang, C.; Song, B.; Chang, C. Terahertz wave accelerates DNA unwinding: A molecular dynamics simulation study. *J. Phys. Chem. Lett.* **2020**, *11* (17), 7002–7008.
- (89) Banerjee, S.; Wilson, J.; Shim, J.; Shankla, M.; Corbin, E. A.; Aksimentiev, A.; Bashir, R. Slowing DNA transport using graphene—DNA interactions. *Adv. Funct. Mater.* **2015**, 25 (6), 936–946.
- (90) Li, N. K.; Kim, H. S.; Nash, J. A.; Lim, M.; Yingling, Y. G. Progress in molecular modelling of DNA materials. *Mol. Simul.* **2014**, 40 (10–11), 777–783.
- (91) Dans, P. D.; Walther, J.; Gómez, H.; Orozco, M. Multiscale simulation of DNA. *Curr. Opin. Struct. Biol.* **2016**, *37*, 29–45.
- (92) Ouldridge, T. E.; Louis, A. A.; Doye, J. P. DNA nanotweezers studied with a coarse-grained model of DNA. *Phys. Rev. Lett.* **2010**, 104 (17), 178101.
- (93) Noid, W. G. Perspective: Coarse-grained models for biomolecular systems. *I. Chem. Phys.* **2013**, *139* (9), No. 090901.
- (94) Sun, T.; Minhas, V.; Korolev, N.; Mirzoev, A.; Lyubartsev, A. P.; Nordenskiöld, L. Bottom-up coarse-grained modeling of DNA. *Frontiers in Molecular Biosciences* **2021**, *8*, 645527.
- (95) Reith, D.; Pütz, M.; Müller-Plathe, F. Deriving effective mesoscale potentials from atomistic simulations. *Journal of computational chemistry* **2003**, 24 (13), 1624–1636.
- (96) Agrawal, V.; Arya, G.; Oswald, J. Simultaneous iterative Boltzmann inversion for coarse-graining of polyurea. *Macromolecules* **2014**, *47* (10), 3378–3389.
- (97) Ercolessi, F.; Adams, J. B. Interatomic potentials from first-principles calculations: the force-matching method. *EPL (Europhysics Letters)* **1994**, 26 (8), 583.
- (98) Shell, M. S. Coarse-graining with the relative entropy. *Advances in chemical physics* **2016**, 395.
- (99) Wang, J.; Olsson, S.; Wehmeyer, C.; Pérez, A.; Charron, N. E.; De Fabritiis, G.; Noé, F.; Clementi, C. Machine learning of coarse-grained molecular dynamics force fields. *ACS central science* **2019**, 5 (5), 755–767.
- (100) Marrink, S. J.; Risselada, H. J.; Yefimov, S.; Tieleman, D. P.; De Vries, A. H. The MARTINI force field: coarse grained model for biomolecular simulations. *J. Phys. Chem. B* **2007**, *111* (27), 7812–7824.
- (101) Sengar, A.; Ouldridge, T. E.; Henrich, O.; Rovigatti, L.; Šulc, P. A primer on the oxDNA model of DNA: when to use it, how to simulate it and how to interpret the results. *Frontiers in Molecular Biosciences* **2021**, *8*, 693710.
- (102) Knotts, T. A., IV; Rathore, N.; Schwartz, D. C.; De Pablo, J. J. A coarse grain model for DNA. *J. Chem. Phys.* **2007**, 126 (8), No. 02B611.
- (103) Savelyev, A.; Papoian, G. A. Chemically accurate coarse graining of double-stranded DNA. *Proc. Natl. Acad. Sci. U. S. A.* **2010**, 107 (47), 20340–20345.
- (104) Shi, Z.; Castro, C. E.; Arya, G. Conformational dynamics of mechanically compliant DNA nanostructures from coarse-grained molecular dynamics simulations. *ACS Nano* **2017**, *11* (5), 4617–4630
- (105) Snodin, B. E.; Romano, F.; Rovigatti, L.; Ouldridge, T. E.; Louis, A. A.; Doye, J. P. Direct simulation of the self-assembly of a small DNA origami. *ACS Nano* **2016**, *10* (2), 1724–1737.

- (106) Huang, C. M.; Kucinic, A.; Johnson, J. A.; Su, H. J.; Castro, C. E. Integrated computer-aided engineering and design for DNA assemblies. *Nat. Mater.* **2021**, *20* (9), 1264–1271.
- (107) Büchl, A.; Kopperger, E.; Vogt, M.; Langecker, M.; Simmel, F. C.; List, J. Energy landscapes of rotary DNA origami devices determined by fluorescence particle tracking. *Biophys. J.* **2022**, *121*, 4849.
- (108) Douglas, S. M.; Marblestone, A. H.; Teerapittayanon, S.; Vazquez, A.; Church, G. M.; Shih, W. M. Rapid prototyping of 3D DNA-origami shapes with caDNAno. *Nucleic acids research* **2009**, 37 (15), 5001–5006.
- (109) Veneziano, R.; Ratanalert, S.; Zhang, K.; Zhang, F.; Yan, H.; Chiu, W.; Bathe, M. Designer nanoscale DNA assemblies programmed from the top down. *Science* **2016**, 352 (6293), 1534–1534.
- (110) Huang, C.-M.; Kucinic, A.; Johnson, J. A.; Su, H.-J.; Castro, C. E. Integrated computer-aided engineering and design for DNA assemblies. *Nat. Mater.* **2021**, *20* (9), 1264–1271.
- (111) Williams, S.; Lund, K.; Lin, C.; Wonka, P.; Lindsay, S.; Yan, H. *Tiamat: A Three-Dimensional Editing Tool for Complex DNA Structures*; International Workshop on DNA-Based Computers; Springer: New York, 2008; pp 90–101.
- (112) Jun, H.; Wang, X.; Parsons, M. F.; Bricker, W. P.; John, T.; Li, S.; Jackson, S.; Chiu, W.; Bathe, M. Rapid prototyping of arbitrary 2D and 3D wireframe DNA origami. *Nucleic acids research* **2021**, 49 (18), 10265–10274.
- (113) Jun, H.; Wang, X.; Bricker, W. P.; Bathe, M. Automated sequence design of 2D wireframe DNA origami with honeycomb edges. *Nat. Commun.* **2019**, *10* (1), 1–9.
- (114) Jun, H.; Zhang, F.; Shepherd, T.; Ratanalert, S.; Qi, X.; Yan, H.; Bathe, M. Autonomously designed free-form 2D DNA origami. *Science advances* **2019**, *5* (1), eaav0655.
- (115) Jun, H.; Shepherd, T. R.; Zhang, K.; Bricker, W. P.; Li, S.; Chiu, W.; Bathe, M. Automated sequence design of 3D polyhedral wireframe DNA origami with honeycomb edges. *ACS Nano* **2019**, *13* (2), 2083–2093.
- (116) Snodin, B. E.; Schreck, J. S.; Romano, F.; Louis, A. A.; Doye, J. P. Coarse-grained modelling of the structural properties of DNA origami. *Nucleic acids research* **2019**, *47* (3), 1585–1597.
- (117) Yang, Y.; Lu, Q.; Huang, C. M.; Qian, H.; Zhang, Y.; Deshpande, S.; Arya, G.; Ke, Y.; Zauscher, S. Programmable Site-Specific Functionalization of DNA Origami with Polynucleotide Brushes. *Angew. Chem., Int. Ed.* **2021**, *60* (43), 23241–23247.
- (118) Zhou, L.; Marras, A. E.; Huang, C. M.; Castro, C. E.; Su, H. J. Paper Origami-Inspired Design and Actuation of DNA Nanomachines with Complex Motions. *Small* **2018**, *14* (47), 1802580.
- (119) DeLuca, M.; Shi, Z.; Castro, C. E.; Arya, G. Dynamic DNA nanotechnology: toward functional nanoscale devices. *Nanoscale Horizons* **2020**, 5 (2), 182–201.
- (120) Shi, Z.; Arya, G. Free energy landscape of salt-actuated reconfigurable DNA nanodevices. *Nucleic acids research* **2020**, 48 (2), 548–560.
- (121) Wang, D.; Yu, L.; Huang, C.-M.; Arya, G.; Chang, S.; Ke, Y. Programmable transformations of DNA origami made of small modular dynamic units. *J. Am. Chem. Soc.* **2021**, *143* (5), 2256–2263.
- (122) Srinivas, N.; Ouldridge, T. E.; Šulc, P.; Schaeffer, J. M.; Yurke, B.; Louis, A. A.; Doye, J. P.; Winfree, E. On the biophysics and kinetics of toehold-mediated DNA strand displacement. *Nucleic acids research* **2013**, 41 (22), 10641–10658.
- (123) Machinek, R. R.; Ouldridge, T. E.; Haley, N. E.; Bath, J.; Turberfield, A. J. Programmable energy landscapes for kinetic control of DNA strand displacement. *Nat. Commun.* **2014**, *5* (1), 1–9.
- (124) Šulc, P.; Ouldridge, T. E.; Romano, F.; Doye, J. P.; Louis, A. A. Modelling toehold-mediated RNA strand displacement. *Biophysical journal* **2015**, *108* (5), 1238–1247.
- (125) Hastings, W. K. Monte Carlo sampling methods using Markov chains and their applications. *Biometrika* **1970**, *57*, 97.

(126) Cumberworth, A.; Frenkel, D.; Reinhardt, A. Simulations of DNA-origami self-assembly reveal design-dependent nucleation barriers. *Nano Lett.* **2022**, 22, 6916–6922.

www.acsabm.org

- (127) Wedemann, G.; Langowski, J. Computer simulation of the 30-nanometer chromatin fiber. *Biophysical journal* **2002**, 82 (6), 2847–2859.
- (128) Arya, G.; Zhang, Q.; Schlick, T. Flexible histone tails in a new mesoscopic oligonucleosome model. *Biophysical journal* **2006**, *91* (1), 133–150.
- (129) Meluzzi, D.; Arya, G. Recovering ensembles of chromatin conformations from contact probabilities. *Nucleic acids research* **2013**, 41 (1), 63–75.
- (130) Di Pierro, M.; Potoyan, D. A.; Wolynes, P. G.; Onuchic, J. N. Anomalous diffusion, spatial coherence, and viscoelasticity from the energy landscape of human chromosomes. *Proc. Natl. Acad. Sci. U. S. A.* **2018**, *115* (30), 7753–7758.
- (131) MacPherson, Q.; Beltran, B.; Spakowitz, A. J. Bottom-up modeling of chromatin segregation due to epigenetic modifications. *Proc. Natl. Acad. Sci. U. S. A.* **2018**, *115* (50), 12739–12744.
- (132) Grigoryev, S. A.; Arya, G.; Correll, S.; Woodcock, C. L.; Schlick, T. Evidence for heteromorphic chromatin fibers from analysis of nucleosome interactions. *Proc. Natl. Acad. Sci. U. S. A.* **2009**, *106* (32), 13317–13322.
- (133) Arya, G.; Schlick, T. Role of histone tails in chromatin folding revealed by a mesoscopic oligonucleosome model. *Proc. Natl. Acad. Sci. U. S. A.* **2006**, *103* (44), 16236–16241.
- (134) Sambriski, E.; Schwartz, D.; De Pablo, J. A mesoscale model of DNA and its renaturation. *Biophysical journal* **2009**, *96* (5), 1675–1690.
- (135) Wang, Y.; Tree, D. R.; Dorfman, K. D. Simulation of DNA extension in nanochannels. *Macromolecules* **2011**, *44* (16), 6594–6604
- (136) Randall, G. C.; Doyle, P. S. DNA deformation in electric fields: DNA driven past a cylindrical obstruction. *Macromolecules* **2005**, 38 (6), 2410–2418.
- (137) Spakowitz, A. J.; Wang, Z.-G. DNA packaging in bacteriophage: is twist important? *Biophysical journal* **2005**, 88 (6), 3912–3923.
- (138) Maffeo, C.; Aksimentiev, A. MrDNA: a multi-resolution model for predicting the structure and dynamics of DNA systems. *Nucleic acids research* **2020**, 48 (9), 5135–5146.
- (139) Ke, Y.; Ong, L. L.; Shih, W. M.; Yin, P. Three-dimensional structures self-assembled from DNA bricks. *science* **2012**, 338 (6111), 1177–1183.
- (140) Reinhardt, A.; Frenkel, D. Numerical evidence for nucleated self-assembly of DNA brick structures. *Physical review letters* **2014**, *112* (23), 238103.
- (141) Rovigatti, L.; Russo, J.; Romano, F.; Matthies, M.; Kroc, L.; Šulc, P. A simple solution to the problem of self-assembling cubic diamond crystals. *Nanoscale* **2022**, *14* (38), 14268–14275.
- (142) Crocker, K.; Johnson, J.; Pfeifer, W.; Castro, C.; Bundschuh, R. A quantitative model for a nanoscale switch accurately predicts thermal actuation behavior. *Nanoscale* **2021**, *13* (32), 13746–13757.
- (143) Ouldridge, T. E. Coarse-Grained Modelling of DNA and DNA Self-Assembly; Springer Science & Business Media: New York, 2012.
- (144) Qian, L.; Winfree, E. Scaling up digital circuit computation with DNA strand displacement cascades. *science* **2011**, 332 (6034), 1196–1201.
- (145) Chandran, H.; Gopalkrishnan, N.; Phillips, A.; Reif, J. Localized hybridization circuits. *International Workshop on DNA-Based Computers*; Springer: New York, 2011; pp 64–83.
- (146) Kumar, S.; Weisburd, J. M.; Lakin, M. R. Structure sampling for computational estimation of localized DNA interaction rates. *Sci. Rep.* **2021**, *11*, 1–14.
- (147) Zhang, D. Y.; Seelig, G. Dynamic DNA nanotechnology using strand-displacement reactions. *Nature Chem.* **2011**, 3 (2), 103–113. (148) Gautam, V.; Long, S.; Orponen, P. RuleDSD: A Rule-based Modelling and Simulation Tool for DNA Strand Displacement Systems. *Bioinformatics* **2020**, 158–167.

- (149) Cardelli, L. Two-domain DNA strand displacement. Mathematical Structures in Computer Science 2013, 23 (2), 247–271.
- (150) Phillips, A.; Cardelli, L. A programming language for composable DNA circuits. *J. R. Soc., Interface* **2009**, *6* (suppl_4), S419–S436.
- (151) Qian, L.; Winfree, E.; Bruck, J. Neural network computation with DNA strand displacement cascades. *nature* **2011**, 475 (7356), 368–372.
- (152) Lakin, M. R.; Youssef, S.; Cardelli, L.; Phillips, A. Abstractions for DNA circuit design. *Journal of The Royal Society Interface* **2012**, *9* (68), 470–486.
- (153) Yordanov, B.; Kim, J.; Petersen, R. L.; Shudy, A.; Kulkarni, V. V.; Phillips, A. Computational design of nucleic acid feedback control circuits. *ACS synthetic biology* **2014**, *3* (8), 600–616.
- (154) Montagne, K.; Plasson, R.; Sakai, Y.; Fujii, T.; Rondelez, Y. Programming an in vitro DNA oscillator using a molecular networking strategy. *Molecular systems biology* **2011**, 7 (1), 466.
- (155) Kim, J.; Winfree, E. Synthetic in vitro transcriptional oscillators. *Molecular systems biology* **2011**, *7* (1), 465.
- (156) Chen, Y.-J.; Dalchau, N.; Srinivas, N.; Phillips, A.; Cardelli, L.; Soloveichik, D.; Seelig, G. Programmable chemical controllers made from DNA. *Nature Nanotechnol.* **2013**, 8 (10), 755–762.
- (157) Fujii, T.; Rondelez, Y. Predator-prey molecular ecosystems. ACS Nano 2013, 7 (1), 27-34.
- (158) Weitz, M.; Kim, J.; Kapsner, K.; Winfree, E.; Franco, E.; Simmel, F. C. Diversity in the dynamical behaviour of a compartmentalized programmable biochemical oscillator. *Nature Chem.* **2014**, *6* (4), 295–302.
- (159) Schaeffer, J. M.; Thachuk, C.; Winfree, E. Stochastic simulation of the kinetics of multiple interacting nucleic acid strands. *International Workshop on DNA-Based Computers*; Springer: New York, 2015; pp 194–211.
- (160) Sensale, S.; Sharma, P.; Arya, G. Binding kinetics of harmonically confined random walkers. *Phys. Rev. E* **2022**, *105* (4), No. 044136.
- (161) Smith, S.; Grima, R. Spatial stochastic intracellular kinetics: A review of modelling approaches. *Bulletin of mathematical biology* **2019**, *81* (8), 2960–3009.
- (162) Arredondo, D.; Stefanovic, D. Effect of polyvalency on tethered molecular walkers on independent one-dimensional tracks. *Phys. Rev. E* **2020**, *101* (6), No. 062101.
- (163) Korosec, C. S.; Zuckermann, M. J.; Forde, N. R. Dimensionality-dependent crossover in motility of polyvalent burnt-bridges ratchets. *Phys. Rev. E* **2018**, 98 (3), No. 032114.
- (164) Kopperger, E.; Pirzer, T.; Simmel, F. C. Diffusive transport of molecular cargo tethered to a DNA origami platform. *Nano Lett.* **2015**, *15* (4), 2693–2699.
- (165) Lakin, M. R.; Youssef, S.; Polo, F.; Emmott, S.; Phillips, A. Visual DSD: a design and analysis tool for DNA strand displacement systems. *Bioinformatics* **2011**, *27* (22), 3211–3213.
- (166) Du, Y.; Pan, J.; Qiu, H.; Mao, C.; Choi, J. H. Mechanistic Understanding of Surface Migration Dynamics with DNA Walkers. *J. Phys. Chem. B* **2021**, *125* (2), 507–517.
- (167) Berleant, J.; Berlind, C.; Badelt, S.; Dannenberg, F.; Schaeffer, J.; Winfree, E. Automated sequence-level analysis of kinetics and thermodynamics for domain-level DNA strand-displacement systems. *J. R. Soc., Interface* **2018**, *15* (149), 20180107.
- (168) Grun, C.; Werfel, J.; Zhang, D. Y.; Yin, P. DyNAMiC Workbench: an integrated development environment for dynamic DNA nanotechnology. J. R. Soc., Interface 2015, 12 (111), 20150580.
- (169) Patitz, M. J. An introduction to tile-based self-assembly and a survey of recent results. *Natural Computing* **2014**, *13*, 195–224.
- (170) Evans, C. G.; Winfree, E. Physical principles for DNA tile self-assembly. *Chem. Soc. Rev.* **2017**, *46* (12), 3808–3829.
- (171) Woo, S.; Rothemund, P. W. Programmable molecular recognition based on the geometry of DNA nanostructures. *Nature Chem.* **2011**, 3 (8), 620–627.

- (172) Liu, W.; Zhong, H.; Wang, R.; Seeman, N. C. Crystalline two-dimensional DNA-origami arrays. *Angew. Chem., Int. Ed.* **2011**, *50* (1), 264–267.
- (173) Petersen, P.; Tikhomirov, G.; Qian, L. Information-based autonomous reconfiguration in systems of interacting DNA nanostructures. *Nat. Commun.* **2018**, *9* (1), 5362.
- (174) Tikhomirov, G.; Petersen, P.; Qian, L. Triangular DNA origami tilings. J. Am. Chem. Soc. 2018, 140 (50), 17361–17364.
- (175) Zhou, C.; Yang, D.; Sensale, S.; Sharma, P.; Wang, D.; Yu, L.; Arya, G.; Ke, Y.; Wang, P. A bistable and reconfigurable molecular system with encodable bonds. *Science Advances* **2022**, *8* (46), eade 3003.
- (176) Winfree, E.; Liu, F.; Wenzler, L. A.; Seeman, N. C. Design and self-assembly of two-dimensional DNA crystals. *Nature* **1998**, 394 (6693), 539–544.
- (177) Fujibayashi, K.; Hariadi, R.; Park, S. H.; Winfree, E.; Murata, S. Toward reliable algorithmic self-assembly of DNA tiles: A fixed-width cellular automaton pattern. *Nano Lett.* **2008**, *8* (7), 1791–1797.
- (178) Schiefer, N.; Winfree, E. Universal computation and optimal construction in the chemical reaction network-controlled tile assembly model. *DNA Computing and Molecular Programming: 21st International Conference, DNA 21*; Boston and Cambridge, MA, August 17–21, 2015, Proceedings 21; Springer: New York, 2015; pp 34–54.
- (179) Schiefer, N.; Winfree, E. Time complexity of computation and construction in the chemical reaction network-controlled tile assembly model. *DNA Computing and Molecular Programming: 22nd International Conference, DNA 22*; Munich, Germany, September 4–8, 2016; Springer: New York, 2016; pp 165–182.
- (180) Green, L. N.; Subramanian, H. K.; Mardanlou, V.; Kim, J.; Hariadi, R. F.; Franco, E. Autonomous dynamic control of DNA nanostructure self-assembly. *Nature Chem.* **2019**, *11* (6), 510–520.
- (181) Amodio, A.; Adedeji, A. F.; Castronovo, M.; Franco, E.; Ricci, F. pH-controlled assembly of DNA tiles. *J. Am. Chem. Soc.* **2016**, *138* (39), 12735–12738.
- (182) Tang, L.; Navarro, L. A., Jr; Chilkoti, A.; Zauscher, S. High-Molecular-Weight Polynucleotides by Transferase-Catalyzed Living Chain-Growth Polycondensation. *Angew. Chem.* **2017**, 129 (24), 6882–6886.
- (183) Dannenberg, F.; Dunn, K. E.; Bath, J.; Kwiatkowska, M.; Turberfield, A. J.; Ouldridge, T. E. Modelling DNA origami self-assembly at the domain level. *J. Chem. Phys.* **2015**, *143*, 2576–6422.
- (184) Chen, H.; Weng, T.-W.; Riccitelli, M. M.; Cui, Y.; Irudayaraj, J.; Choi, J. H. Understanding the mechanical properties of DNA origami tiles and controlling the kinetics of their folding and unfolding reconfiguration. *J. Am. Chem. Soc.* **2014**, *136* (19), 6995–7005.
- (185) Arbona, J.-M.; Aimé, J.-P.; Elezgaray, J. Cooperativity in the annealing of DNA origamis. *J. Chem. Phys.* **2013**, *138* (1), No. 01B606.
- (186) Cumberworth, A.; Reinhardt, A.; Frenkel, D. Lattice models and Monte Carlo methods for simulating DNA origami self-assembly. *J. Chem. Phys.* **2018**, *149* (23), 234905.
- (187) Klinge, T. H.; Lathrop, J. I.; Moreno, S.; Potter, H. D.; Raman, N. K.; Riley, M. R. ALCH: an imperative language for chemical reaction network-controlled tile assembly. *Natural Computing* **2022**, 1–21.
- (188) Alumbaugh, J. C.; Daymude, J. J.; Demaine, E. D.; Patitz, M. J.; Richa, A. W. Simulation of programmable matter systems using active tile-based self-assembly. *International Conference on DNA Computing and Molecular Programming*; Springer: New York, 2019; pp 140–158.
- (189) Castro, C. E.; Kilchherr, F.; Kim, D. N.; Shiao, E. L.; Wauer, T.; Wortmann, P.; Bathe, M.; Dietz, H. A primer to scaffolded DNA origami. *Nat. Methods* **2011**, *8* (3), 221–9.
- (190) Lee, J. Y.; Lee, J. G.; Yun, G.; Lee, C.; Kim, Y.-J.; Kim, K. S.; Kim, T. H.; Kim, D.-N. Rapid computational analysis of DNA origami assemblies at near-atomic resolution. *ACS Nano* **2021**, *15* (1), 1002–1015.

- (191) Tian, Y.; Lhermitte, J. R.; Bai, L.; Vo, T.; Xin, H. L.; Li, H.; Li, R.; Fukuto, M.; Yager, K. G.; Kahn, J. S. Ordered three-dimensional nanomaterials using DNA-prescribed and valence-controlled material voxels. *Nature materials* **2020**, *19* (7), 789–796.
- (192) Wintersinger, C. M.; Minev, D.; Ershova, A.; Sasaki, H. M.; Gowri, G.; Berengut, J. F.; Corea-Dilbert, F. E.; Yin, P.; Shih, W. M. Multi-micron crisscross structures grown from DNA-origami slats. *Nat. Nanotechnol.* **2022**, 1–9.
- (193) Castro, C. E.; Su, H.-J.; Marras, A. E.; Zhou, L.; Johnson, J. Mechanical design of DNA nanostructures. *Nanoscale* **2015**, *7* (14), 5913–5921.
- (194) Procyk, J.; Poppleton, E.; Sulc, P. Coarse-grained nucleic acid-protein model for hybrid nanotechnology. *Soft Matter* **2021**, *17* (13), 3586–3593.
- (195) Fonseca, P.; Romano, F.; Schreck, J. S.; Ouldridge, T. E.; Doye, J. P.; Louis, A. A. Multi-scale coarse-graining for the study of assembly pathways in DNA-brick self-assembly. *J. Chem. Phys.* **2018**, 148 (13), 134910.
- (196) Wang, C.; Huang, W.; Liao, J.-L. QM/MM investigation of ATP hydrolysis in aqueous solution. *J. Phys. Chem. B* **2015**, *119* (9), 3720–3726.
- (197) Ahmadi, S.; Barrios Herrera, L.; Chehelamirani, M.; Hostaš, J.; Jalife, S.; Salahub, D. R. Multiscale modeling of enzymes: QM-cluster, QM/MM, and QM/MM/MD: a tutorial review. *Int. J. Quantum Chem.* **2018**, *118* (9), e25558.
- (198) Kuzyk, A.; Jungmann, R.; Acuna, G. P.; Liu, N. DNA origami route for nanophotonics. *ACS photonics* **2018**, *5* (4), 1151–1163.
- (199) Chen, C.; Wei, X.; Parsons, M. F.; Guo, J.; Banal, J. L.; Zhao, Y.; Scott, M. N.; Schlau-Cohen, G. S.; Hernandez, R.; Bathe, M. Nanoscale 3D spatial addressing and valence control of quantum dots using wireframe DNA origami. *Nat. Commun.* **2022**, *13* (1), 1–15.
- (200) Bui, H.; Onodera, C.; Kidwell, C.; Tan, Y.; Graugnard, E.; Kuang, W.; Lee, J.; Knowlton, W. B.; Yurke, B.; Hughes, W. L. Programmable periodicity of quantum dot arrays with DNA origami nanotubes. *Nano Lett.* **2010**, *10* (9), 3367–3372.
- (201) Huang, D.; Freeley, M.; Palma, M. DNA-mediated patterning of single quantum dot nanoarrays: A reusable platform for single-molecule control. *Sci. Rep.* **2017**, *7* (1), 1–7.
- (202) David, C. C.; Jacobs, D. J. Principal component analysis: a method for determining the essential dynamics of proteins. *Methods Mol. Biol.* **2014**, *1084*, 193–226.
- (203) Poppleton, E.; Bohlin, J.; Matthies, M.; Sharma, S.; Zhang, F.; Šulc, P. Design, optimization and analysis of large DNA and RNA nanostructures through interactive visualization, editing and molecular simulation. *Nucleic acids research* **2020**, 48 (12), e72–e72.
- (204) Chhabra, H.; Mishra, G.; Cao, Y.; Prešern, D.; Skoruppa, E.; Tortora, M. M.; Doye, J. P. Computing the elastic mechanical properties of rodlike DNA nanostructures. *J. Chem. Theory Comput.* **2020**, *16* (12), 7748–7763.
- (205) Kroon-Batenburg, L. M.; Kruiskamp, P. H.; Vliegenthart, J. F.; Kroon, J. Estimation of the persistence length of polymers by MD simulations on small fragments in solution. Application to cellulose. *J. Phys. Chem. B* **1997**, *101* (42), 8454–8459.
- (206) Brinkers, S.; Dietrich, H. R.; de Groote, F. H.; Young, I. T.; Rieger, B. The persistence length of double stranded DNA determined using dark field tethered particle motion. *J. Chem. Phys.* **2009**, *130* (21), No. 06B607.
- (207) Einstein, A. Über die von der molekularkinetischen Theorie der Wärme geforderte Bewegung von in ruhenden Flüssigkeiten suspendierten Teilchen. *Annalen der physik* **1905**, *4*, 549.
- (208) Ermak, D. L.; McCammon, J. A. Brownian dynamics with hydrodynamic interactions. *J. Chem. Phys.* **1978**, *69* (4), 1352–1360. (209) Kaufhold, W. T.; Pfeifer, W.; Castro, C. E.; Di Michele, L. Probing the mechanical properties of DNA nanostructures with metadynamics. *ACS Nano* **2022**, *16*, 8784.
- (210) Yang, Y. I.; Shao, Q.; Zhang, J.; Yang, L.; Gao, Y. Q. Enhanced sampling in molecular dynamics. *J. Chem. Phys.* **2019**, *151* (7), No. 070902.

- (211) Grossfield, A. WHAM: The Weighted Histogram Analysis Method, version 2.0.11; http://membrane.urmc.rochester.edu/wordpress/?page_id=126, 2022.
- (212) Laio, A.; Gervasio, F. L. Metadynamics: a method to simulate rare events and reconstruct the free energy in biophysics, chemistry and material science. *Rep. Prog. Phys.* **2008**, *71* (12), 126601.
- (213) Fiorin, G.; Pastore, A.; Carloni, P.; Parrinello, M. Using metadynamics to understand the mechanism of calmodulin/target recognition at atomic detail. *Biophys. J.* **2006**, *91* (8), 2768–2777.
- (214) Biswas, M.; Lickert, B.; Stock, G. Metadynamics enhanced Markov modeling of protein dynamics. *J. Phys. Chem. B* **2018**, 122 (21), 5508–5514.
- (215) Limongelli, V.; Bonomi, M.; Parrinello, M. Funnel metadynamics as accurate binding free-energy method. *Proc. Natl. Acad. Sci. U. S. A.* **2013**, *110* (16), 6358–6363.
- (216) Yang, Y.; Lu, Q.; Huang, C. M.; Qian, H.; Zhang, Y.; Deshpande, S.; Arya, G.; Ke, Y.; Zauscher, S. Programmable Site-Specific Functionalization of DNA Origami with Polynucleotide Brushes. *Angew. Chem.* **2021**, *133* (43), 23429–23435.
- (217) Mirkin, C. A.; Letsinger, R. L.; Mucic, R. C.; Storhoff, J. J. A DNA-based method for rationally assembling nanoparticles into macroscopic materials. *Nature* **1996**, 382 (6592), 607–609.
- (218) Nykypanchuk, D.; Maye, M. M.; Van Der Lelie, D.; Gang, O. DNA-guided crystallization of colloidal nanoparticles. *Nature* **2008**, 451 (7178), 549–552.
- (219) Bartnik, K.; Barth, A.; Pilo-Pais, M.; Crevenna, A. H.; Liedl, T.; Lamb, D. C. A DNA Origami Platform for Single-Pair Förster Resonance Energy Transfer Investigation of DNA–DNA Interactions and Ligation. *J. Am. Chem. Soc.* **2020**, *142* (2), 815–825.
- (220) Barbas, C. F.; Burton, D. R.; Scott, J. K.; Silverman, G. J. Quantitation of DNA and RNA. *Cold Spring Harbor Protocols* **2007**, 2007 (11), pdb.ip47.
- (221) McCarte, B.; Yeung, O. T.; Speakman, A. J.; Elfick, A.; Dunn, K. E. Using ultraviolet absorption spectroscopy to study nanoswitches based on non-canonical DNA structures. *Biochemistry and Biophysics Reports* **2022**, *31*, 101293.
- (222) Li, H.; Rothberg, L. Colorimetric detection of DNA sequences based on electrostatic interactions with unmodified gold nanoparticles. *Proc. Natl. Acad. Sci. U. S. A.* **2004**, *101* (39), 14036–14039. (223) Cheon, H.; Yang, H.-j.; Lee, S.-H.; Kim, Y. A.; Son, J.-H. Terahertz molecular resonance of cancer DNA. *Sci. Rep.* **2016**, *6* (1), 1–10
- (224) Brown, E.; Mendoza, E.; Kuznetsova, Y.; Neumann, A.; Brueck, S. THz signatures of DNA in nanochannels under electrophoretic control. *Sensors* **2013**, 1–3.
- (225) Sun, L.; Zhao, L.; Peng, R.-Y. Research progress in the effects of terahertz waves on biomacromolecules. *Military Medical Research* **2021**, *8*, 1–8.
- (226) Globus, T.; Woolard, D.; Bykhovskaia, M.; Gelmont, B.; Werbos, L.; Samuels, A. THz-frequency spectroscopic sensing of DNA and related biological materials. *International Journal of High Speed Electronics and Systems* **2003**, *13* (04), 903–936.
- (227) Tang, M.; Zhang, M.; Yan, S.; Xia, L.; Yang, Z.; Du, C.; Cui, H.-L.; Wei, D. Detection of DNA oligonucleotides with base mutations by terahertz spectroscopy and microstructures. *PloS one* **2018**, *13* (1), No. e0191515.
- (228) Zhang, C.; Yuan, Y.; Wu, K.; Wang, Y.; Zhu, S.; Shi, J.; Wang, L.; Li, Q.; Zuo, X.; Fan, C. Driving DNA origami assembly with a terahertz wave. *Nano Lett.* **2022**, *22*, 468–475.
- (229) Shah, S. I. H.; Lim, S. Review on recent origami inspired antennas from microwave to terahertz regime. *Materials & Design* **2021**, 198, 109345.
- (230) Tapio, K.; Mostafa, A.; Kanehira, Y.; Suma, A.; Dutta, A.; Bald, I. A Versatile DNA Origami-Based Plasmonic Nanoantenna for Label-Free Single-Molecule Surface-Enhanced Raman Spectroscopy. *ACS Nano* **2021**, *15* (4), 7065–7077.
- (231) Yao, S.; Georgakopoulos, S. V.; Cook, B.; Tentzeris, M. A novel reconfigurable origami accordion antenna. 2014 IEEE MTT-S

- International Microwave Symposium (IMS2014); IEEE: New York, 2014; pp 1-4.
- (232) Bricker, W. P.; Shenai, P. M.; Ghosh, A.; Liu, Z.; Enriquez, M. G. M.; Lambrev, P. H.; Tan, H.-S.; Lo, C. S.; Tretiak, S.; Fernandez-Alberti, S. Non-radiative relaxation of photoexcited chlorophylls: theoretical and experimental study. *Sci. Rep.* **2015**, *5* (1), 1–16.
- (233) Yi, W.; Yu, J.; Xu, Y.; Wang, F.; Yu, Q.; Sun, H.; Xu, L.; Liu, Y.; Jiang, L. Broadband terahertz spectroscopy of amino acids. *Instrumentation Science & Technology* **2017**, 45 (4), 423–439.
- (234) Thomas, M.; Brehm, M.; Fligg, R.; Vöhringer, P.; Kirchner, B. Computing vibrational spectra from ab initio molecular dynamics. *Phys. Chem. Phys.* **2013**, *15* (18), 6608–6622.
- (235) Nicolaï, A.; Delarue, P.; Senet, P. Low-frequency, functional, modes of proteins: all-atom and coarse-grained normal mode analysis. Computational Methods to Study the Structure and Dynamics of Biomolecules and Biomolecular Processes; Springer: New York, 2014; pp 483–524.
- (236) Adrian, M.; Dubochet, J.; Lepault, J.; McDowall, A. W. Cryoelectron microscopy of viruses. *Nature* **1984**, 308 (5954), 32–36.
- (237) Murata, K.; Wolf, M. Cryo-electron microscopy for structural analysis of dynamic biological macromolecules. *Biochimica et Biophysica Acta (BBA)-General Subjects* **2018**, *1862* (2), 324–334.
- (238) Zhao, S.; Tian, R.; Wu, J.; Liu, S.; Wang, Y.; Wen, M.; Shang, Y.; Liu, Q.; Li, Y.; Guo, Y. A DNA origami-based aptamer nanoarray for potent and reversible anticoagulation in hemodialysis. *Nat. Commun.* **2021**, *12*, 1–10.
- (239) Wang, S.-T.; Gray, M. A.; Xuan, S.; Lin, Y.; Byrnes, J.; Nguyen, A. I.; Todorova, N.; Stevens, M. M.; Bertozzi, C. R.; Zuckermann, R. N. DNA origami protection and molecular interfacing through engineered sequence-defined peptoids. *Proc. Natl. Acad. Sci. U. S. A.* 2020, 117, 6339–6348.
- (240) Silvester, E.; Vollmer, B.; Pražák, V.; Vasishtan, D.; Machala, E. A.; Whittle, C.; Black, S.; Bath, J.; Turberfield, A. J.; Grünewald, K. DNA origami signposts for identifying proteins on cell membranes by electron cryotomography. *Cell* **2021**, *184*, 1110–1121. e16.
- (241) Perrin, F. Mouvement brownien d'un ellipsoide-I Dispersion diélectrique pour des molécules ellipsoidales. *J. phys. radium* **1934**, *5* (10), 497–511.
- (242) Tirado, M. M.; Martínez, C. L.; de la Torre, J. G. Comparison of theories for the translational and rotational diffusion coefficients of rod-like macromolecules. Application to short DNA fragments. *J. Chem. Phys.* **1984**, *81* (4), 2047–2052.
- (243) Doi, M.; Edwards, S. F.; Edwards, S. F. *The Theory of Polymer Dynamics*; Oxford University Press: Oxford, England, 1988; Vol. 73. (244) Cheng, H. F.; Wang, S.; Mirkin, C. A. Electron-Equivalent
- Valency through Molecularly Well-Defined Multivalent DNA. J. Am. Chem. Soc. 2021, 143 (4), 1752–1757.
- (245) Bruetzel, L. K.; Gerling, T.; Sedlak, S. M.; Walker, P. U.; Zheng, W.; Dietz, H.; Lipfert, J. Conformational changes and flexibility of DNA devices observed by small-angle X-ray scattering. *Nano Lett.* **2016**, *16* (8), 4871–4879.
- (246) Fernandez-Castanon, J.; Bomboi, F.; Rovigatti, L.; Zanatta, M.; Paciaroni, A.; Comez, L.; Porcar, L.; Jafta, C. J.; Fadda, G. C.; Bellini, T. Small-angle neutron scattering and molecular dynamics structural study of gelling DNA nanostars. *J. Chem. Phys.* **2016**, *145* (8), No. 084910.
- (247) Vangaveti, S.; D'Esposito, R.; Lippens, J.; Fabris, D.; Ranganathan, S. A coarse-grained model for assisting the investigation of structure and dynamics of large nucleic acids by ion mobility spectrometry—mass spectrometry. *Phys. Chem. Chem. Phys.* **2017**, *19* (23), 14937—14946.
- (248) Lei, D.; Marras, A. E.; Liu, J.; Huang, C.-M.; Zhou, L.; Castro, C. E.; Su, H.-J.; Ren, G. Three-dimensional structural dynamics of DNA origami Bennett linkages using individual-particle electron tomography. *Nat. Commun.* **2018**, *9* (1), 1–8.
- (249) Carleo, G.; Cirac, I.; Cranmer, K.; Daudet, L.; Schuld, M.; Tishby, N.; Vogt-Maranto, L.; Zdeborová, L. Machine learning and the physical sciences. *Rev. Mod. Phys.* **2019**, *91* (4), No. 045002.

- (250) Karniadakis, G. E.; Kevrekidis, I. G.; Lu, L.; Perdikaris, P.; Wang, S.; Yang, L. Physics-informed machine learning. *Nature Reviews Physics* **2021**, *3* (6), 422–440.
- (251) Angermueller, C.; Pärnamaa, T.; Parts, L.; Stegle, O. Deep learning for computational biology. *Molecular systems biology* **2016**, *12* (7), 878.
- (252) Zitnik, M.; Nguyen, F.; Wang, B.; Leskovec, J.; Goldenberg, A.; Hoffman, M. M. Machine learning for integrating data in biology and medicine: Principles, practice, and opportunities. *Information Fusion* **2019**, *50*, 71–91.
- (253) Butler, K. T.; Davies, D. W.; Cartwright, H.; Isayev, O.; Walsh, A. Machine learning for molecular and materials science. *Nature* **2018**, 559 (7715), 547–555.
- (254) Himanen, L.; Geurts, A.; Foster, A. S.; Rinke, P. Data-driven materials science: status, challenges, and perspectives. *Advanced Science* **2019**, *6* (21), 1900808.
- (255) Snoek, J.; Larochelle, H.; Adams, R. P. Practical bayesian optimization of machine learning algorithms. *Adv. Neural Information Processing Syst.* **2012**, *25*, 2951–2959.
- (256) Igel, C.; Hansen, N.; Roth, S. Covariance matrix adaptation for multi-objective optimization. *Evolutionary computation* **2007**, *15* (1), 1–28.
- (257) Rumelhart, D. E.; Hinton, G. E.; Williams, R. J. Learning representations by back-propagating errors. *nature* **1986**, 323 (6088), 533–536.
- (258) Xu, D.; Tian, Y. A comprehensive survey of clustering algorithms. *Annals of Data Science* **2015**, 2 (2), 165–193.
- (259) Hastie, T.; Tibshirani, R.; Friedman, J. H.; Friedman, J. H. *The Elements of Statistical Learning: Data Mining, Inference, and Prediction*; Springer: New York, 2009; Vol. 2.
- (260) Greener, J. G.; Kandathil, S. M.; Moffat, L.; Jones, D. T. A guide to machine learning for biologists. *Nat. Rev. Mol. Cell Biol.* **2022**, 23 (1), 40–55.
- (261) Pandey, R.; Purohit, H.; Castillo, C.; Shalin, V. L. Modeling and mitigating human annotation errors to design efficient stream processing systems with human-in-the-loop machine learning. *International Journal of Human-Computer Studies* **2022**, *160*, 102772.
- (262) Zhang, S.; Jafari, O.; Nagarkar, P. A survey on machine learning techniques for auto labeling of video, audio, and text data, 2021
- (263) Hasan, M.; Kotov, A.; Carcone, A. I.; Dong, M.; Naar, S.; Hartlieb, K. B. A study of the effectiveness of machine learning methods for classification of clinical interview fragments into a large number of categories. *Journal of biomedical informatics* **2016**, *62*, 21–31
- (264) Redmon, J.; Divvala, S.; Girshick, R.; Farhadi, A. You only look once: Unified, real-time object detection. *Proceedings of the IEEE Conference on Computer Vision and Pattern Recognition*, 2016; pp 779–788.
- (265) Chiriboga, M.; Green, C. M.; Hastman, D. A.; Mathur, D.; Wei, Q.; Díaz, S. A.; Medintz, I. L.; Veneziano, R. Rapid DNA origami nanostructure detection and classification using the YOLOv5 deep convolutional neural network. *Sci. Rep.* **2022**, *12*, 1–13.
- (266) Kim, Y. J.; Lim, J.; Kim, D. N. Accelerating AFM Characterization via Deep-Learning-Based Image Super-Resolution. *Small* **2022**, *18* (3), 2103779.
- (267) Auer, A.; Strauss, M. T.; Strauss, S.; Jungmann, R. nanoTRON: a Picasso module for MLP-based classification of super-resolution data. *Bioinformatics* **2020**, *36* (11), 3620–3622.
- (268) Schnitzbauer, J.; Strauss, M. T.; Schlichthaerle, T.; Schueder, F.; Jungmann, R. Super-resolution microscopy with DNA-PAINT. *Nature protocols* **2017**, *12* (6), 1198–1228.
- (269) Zhu, M.; Zhang, L.; Jin, L.; Chen, J.; Zhang, Y.; Xu, Y. DNA-PAINT Imaging Accelerated by Machine Learning. Frontiers in Chemistry 2022, 10, 1.
- (270) Snodin, B. E.; Randisi, F.; Mosayebi, M.; Šulc, P.; Schreck, J. S.; Romano, F.; Ouldridge, T. E.; Tsukanov, R.; Nir, E.; Louis, A. A. Introducing improved structural properties and salt dependence into a

ACS Applied Bio Materials

- coarse-grained model of DNA. *J. Chem. Phys.* **2015**, *142* (23), No. 06B613 1.
- (271) Benson, E.; Lolaico, M.; Tarasov, Y.; Gådin, A.; Högberg, B. r. Evolutionary refinement of DNA nanostructures using coarse-grained molecular dynamics simulations. *ACS Nano* **2019**, *13* (11), 12591–12598.
- (272) Lee, A. J.; Rackers, J. A.; Bricker, W. P. Predicting accurate ab initio DNA electron densities with equivariant neural networks. *Biophys. J.* **2022**, *121* (20), 3883–3895.
- (273) Klein, W. P.; Rolczynski, B. S.; Oliver, S. M.; Zadegan, R.; Buckhout-White, S.; Ancona, M. G.; Cunningham, P. D.; Melinger, J. S.; Vora, P. M.; Kuang, W. DNA origami chromophore scaffold exploiting HomoFRET energy transport to create molecular photonic wires. ACS Applied Nano Materials 2020, 3 (4), 3323–3336.
- (274) Chen, T.; Guestrin, C. Xgboost: A scalable tree boosting system. Proceedings of the 22nd acm sigkdd International Conference on Knowledge Discovery and Data Mining, 2016; pp 785–794.
- (275) Pan, V.; Wang, W.; Heaven, I.; Bai, T.; Cheng, Y.; Chen, C.; Ke, Y.; Wei, B. Monochromatic Fluorescent Barcodes Hierarchically Assembled from Modular DNA Origami Nanorods. *ACS Nano* **2021**, *15* (10), 15892–15901.
- (276) Marras, A.; Zhou, L.; Kolliopoulos, V.; Su, H.; Castro, C. Directing folding pathways for multi-component DNA origami nanostructures with complex topology. *New J. Phys.* **2016**, *18* (5), No. 055005.
- (277) Douglas, S. M.; Dietz, H.; Liedl, T.; Högberg, B.; Graf, F.; Shih, W. M. Self-assembly of DNA into nanoscale three-dimensional shapes. *Nature* **2009**, 459 (7245), 414–418.
- (278) Korolev, N.; Luo, D.; Lyubartsev, A. P.; Nordenskiöld, L. A coarse-grained DNA model parameterized from atomistic simulations by inverse Monte Carlo. *Polymers* **2014**, *6* (6), 1655–1675.
- (279) Jumper, J.; Evans, R.; Pritzel, A.; Green, T.; Figurnov, M.; Ronneberger, O.; Tunyasuvunakool, K.; Bates, R.; Žídek, A.; Potapenko, A. Highly accurate protein structure prediction with AlphaFold. *Nature* **2021**, *596* (7873), 583–589.
- (280) Burley, S. K.; Bhikadiya, C.; Bi, C.; Bittrich, S.; Chao, H.; Chen, L.; Craig, P. A.; Crichlow, G. V.; Dalenberg, K.; Duarte, J. M. RCSB Protein Data Bank: Tools for visualizing and understanding biological macromolecules in 3D. *Protein Sci.* **2022**, *31*, e4482.
- (281) Poppleton, E.; Mallya, A.; Dey, S.; Joseph, J.; Šulc, P. Nanobase. org: a repository for DNA and RNA nanostructures. *Nucleic acids research* **2022**, *50* (D1), D246–D252.